Investigating the role of task intensity on motor unit fatigue recovery

by

Sanjay Veerasammy

A thesis

presented to the University of Waterloo

in fulfillment of the

thesis requirement for the degree of

Master of Science

in

Kinesiology

Waterloo, Ontario, Canada, 2022

Author's Declaration

I hereby declare that I am the sole author of this thesis. This is a true copy of the thesis , including any required final revisions, as accepted by my examiners.

I understand that my thesis may be electronically available to the public.

Abstract

Muscle fatigue-related Musculoskeletal Disorders (MSD) result in millions of dollars of losses annually in North America (Cavuoto, 2016). However, a lack of access to muscle fatigue assessment tools (Enoka & Duchateau, 2016), as well as gaps in our understanding of muscle fatigue recovery (Veerasammy et al., 2022), have limited practitioners' ability to assess and control worker muscle fatigue exposure. Furthermore, it is unclear to what extent the intensity as well as the underlying contributions of larger versus smaller motor units of a performed task impacts the level of fatigue accumulation and recovery. To further develop our knowledge this thesis tested two hypotheses: that the normalized force response (NFR) at each time point would be greater following the high intensity versus low intensity task, indicating that recovery is greater following fatigue at a higher intensity of effort; and, that the NFR at each time point would be greater following the 100Hz stimulation compared to the 20Hz stimulation, indicating that longer term, low-frequency frequency fatigue (Jones, 1996) had occurred.

Twenty-eight healthy right-handed participants (fourteen males, fourteen females) performed a high (70% of their Maximum Voluntary Force (MVF)) and low (20%MVF) intensity isometric 90^{o} elbow extension until task failure. These protocols were performed one week apart, and the order of performance was block randomized. Recovery was then measured as the force produced following muscle electrical stimulation at high (100Hz) and low (20Hz) frequencies. The force outputs were normalized relative to baseline measures. Recovery measures were recorded over the course of one hour following task failure.

A three-factor repeated measures Analysis of Variance (ANOVA) found that significant interaction effects existed between intensity and time ($F(6.0,162.8) = 12.94$, $p < 0.001$, $\eta_p^2 =$

0.32), and between frequency and time ($F(8.64,233.29) = 6.92$, $p < 0.001$, $\eta_p^2 = 0.20$). Post-hoc pair wise comparisons to decompose the intensity by time interaction revealed that the NFR (collapsed across stimulation frequency) was initially higher (0-4 minutes) following the high intensity protocol relative to the low intensity protocol, but then declined and was lower than the NFR following the low intensity protocol (from 10-40 minutes) before returning to a similar NFR as the recovery time approached 60 minutes, with the NFR significantly different at minutes 35 and 60. In contrast, post-hoc pairwise comparisons to decompose the frequency by time interaction revealed that the NFR (collapsed across task intensity) remained higher from minutes 0-60 following high frequency stimulation compared to low frequency stimulation.

From these results, I determined that the higher intensity task caused a greater initial recovery of NFR when compared to recovery from the same task performed at a lower intensity. However, the NFR underwent a force depression following the initial recovery, such that the NFR remained significantly lower following fatigue caused by a high intensity relative to low intensity isometric contraction for up to thirty minutes following task failure. I also noted that the recruited motor units required a higher stimulation frequency to generate forces that were closer to baseline levels at the same input voltage, independent of the intensity of task performed. This indicated that long-term low frequency mechanisms characteristic of smaller motor unit fatigue accumulation (Fuglevand et al., 1999; Jones, 1996) may have similarly contributed to both high and low intensity fatigue recovery profiles. Overall, these findings suggest that muscle fatigue from a sustained isometric contraction may continue to accumulate even after the fatiguing stimulus has been removed. These findings also suggest that overall recovery may be driven by the amount of fatigue accumulated in smaller motor units. Both findings should be considered when informing models that measure muscle fatigue accumulation and recovery.

Acknowledgements

Dr. Steve Fischer, thank you. You took a chance on an international student with more heart than experience. I am thankful for the opportunity you have given me, and for all of the advice, wisdom, and kind words you have imparted.

Dr. Jim Potvin and Dr. Russ Tupling, thank you. You lent invaluable expertise on this thesis but more importantly, taught me that some of the biggest giants in this massive field of Kinesiology are also some of the kindest.

To Dr. Sean Meehan, thank you. For helping me find the right equipment, to teaching me statistics (both formally and informally), and just having an open door and a friendly face.

To Jeff Rice, thank you. This experiment would have never made it off the ground if it wasn't for your engineering expertise.

To my team at the Occupational Biomechanics and Ergonomics Lab (Anna Guenther, Hailey Nestor, Amanda Calford, Dan Armstrong, Justin Davidson, Chris Moore, Sheldon Hawley, Nathalie Oomen, Kate Posluszny, Will Zhao, Daphne Ho, and Alex Malone), a massive thank you. I am so grateful to have spent my undergraduate and graduate degree around you amazing people. From listening to me vent about MATLAB, to giving me advice (both professional and personal), to shocking triceps (thanks Anna and Hailey), and just being all-around good people, I couldn't have done it without you all.

To Tom Hoshizaki, David Varandas, Abhishesh Homagain, Jacklyn Kurt, and Sukirat Bhullar, thank you. A graduate degree is hard, but your shenanigans made it bearable. From giving me a place to live, teaching me how to drive, surviving courses, late nights, and battling for my desk, you all never failed to make me laugh.

To Jean Napenas, Catarina Nascimento, George Gibson, Seanthel Delos Santos, Angela Fu, Ayushi Raval, David Rene, Aiman Fatima, Ruah Alsaghier, Diya Chowdhury, and Gisele Garcia, thank you. It's hard for an international student to make friends in undergrad. I lucked into finding the best friends in the world. Thank you for the debates, the cottage trips, the secret Santas, the last minute study sessions, the board games, the ups, the downs, and the all-arounds.

To David Clusiault and Nikki Ahmadi, thank you. David, thank you for being a brother through the bad times and good times, and for continuing to push me towards being the best version of myself.

To Annie Rupchand, thank you for seeing potential in me that I couldn't see in myself, and for being the gold standard of excellence that I will always strive towards.

To my grandparents, Lily Dutt, Jerry Dutt, Selis Veerasammy, and Edward Veerasammy, that used their life savings so that I could get an undergraduate education. Thank you for taking a chance on me.

To my mother, Liloutie Veerasammy and my father, Harold Veerasammy, who raised me into the man I am today. It was not easy to let me go thousands of miles away to find life on my own. Thank you for your sacrifice and for your endless love.

To my brothers, Aaron Veerasammy and Keenan Veerasammy, thank you for being my lights in some of my darkest moments.

To Helena Nascimento, thank you. For being my best friend, and my rock.

Table of Contents

Author's Declaration ii

Abstract iii

Acknowledgements v

List of Figures ix

List of Tables xii

List of Equations xiii

1.0 Introduction 1

2.0 Literature Review 4

2.1 Integration of muscle fatigue models towards ergonomics assessments 4
2.2 Muscle Motor Unit Properties and Activation 6
2.2.1 Skeletal Muscle Properties 6
2.2.2 Motor Unit Properties and Force Generation 8
2.2.3 Motor Unit Fatigue 10
2.2.5 Motor Unit Fatigue Recovery 13
2.3 Measuring Muscle Fatigue and Recovery 14
2.3.1 Surface Electromyography 14
2.3.2 Muscle Electrical Stimulation 16
2.3.3 The SPiTFiRe Model 23

3.0 Methodology 28

3.1 Simulation of Fatigue from High and Low Intensity Tasks 28
3.2 Experimental Methods 33
3.2.1 Experimental Design 33
3.2.2 Participants 34
3.2.2 Instrumentation 35
3.2.2.1 Force Transducer 35
3.2.2.2 Electromyography 36
3.2.2.3 Muscle Stimulation 38

3.1.3 Protocol **40**
3.3 Data Conditioning **44**
3.4. Statistical Analyses **47**
4.0 Results **48**
4.1 Summary of Participant Performance **48**
4.2 Triceps Force Response to Electrical Stimulation Following Task Failure **50**
4.3 Muscle Activation Characteristics **52**
5.0 Discussion **55**
References **62**
Appendix **68**
Appendix A: Get Active Questionnaire **68**
Appendix B: Nordic Musculoskeletal Questionnaire **70**
Appendix C: Absolute and Normalized Overall Mean Force Responses **71**
Appendix D: Detailed Statistical Results from Pairwise Comparisons **73**
Appendix E: Average NFR across all frequencies and intensities **77**
Appendix F: Percent activation across high and low intensity protocols **78**

List of Figures

Figure 1. Summary of tools and models addressing either Cumulative Mechanical Loading or Muscle Metabolic Fatigue based on their internal tissue mechanism of loading. 5

Figure 2. Skeletal muscle properties (Frontera and Ochala, 2015). 7

Figure 3. The arrangement of motor units. Groups of somatic motor neurons extend from the spinal cord and synapse onto a group of muscle fibers (Silverthorn, 2007). 8

Figure 4. The increasing motor unit size increases their threshold of excitation, force generating capacity, and fatigability 10

Figure 5. Mechanisms of Peripheral Fatigue (Allen et al, 2008) 12

Figure 6. Diagram displaying the increase in muscle EMG activity to maintain a prolonged target force(left) and the subsequent drop-off when the target force cannot be sustained by the largest motor units (right) (Bigland-Ritchie, 1981). 15

Figure 7. Assessing level of recovery through an MVF preferentially assesses the fatigue and recovery of larger motor units, as illustrated using the SPiTFiRe. 17

Figure 8. Typical relationship between voluntary tension and tetanic tension to assess reserve capacity of thumb adductor; the greater the voluntary tension, the lower the contribution from the tetanic tension (Vøllestad, 1997). 18

Figure 9. Visualization of how changing the stimulus intensity (mA) and frequency (Hz) from a muscle stimulator changes the intensity of muscle contractions (%MVC), represented by the dotted black (unfatigued) and solid grey (fatigued) lines. 19

Figure 10. Simulated muscle force response at baseline (A) and recovery following fatigue at high (B) and low (C) intensities. The muscle would have been electrically stimulated at high (100Hz) and low (20Hz) frequencies, and the average expected to be found (D). 20

Figure 11. The overlap between EMG, evoked tetanic force through muscle stimulation, MVC, and the underlying neuromechanical processes resulting in muscle fatigue.. EMG: Electromyography; MVC: Maximum Voluntary Contraction (adapted from Vøllestad, 1997). 22

Figure 12. Flowchart of SPiTFiRe model processing 23

Figure 13. Difference in recovery rates from high and low intensity fatigue 26

Figure 14. Simulated decline and recovery in relative force generating capacity of muscle motor units during the sustained 70 %MVF (A) and the 20% MVF (B) protocols. 30

Figure 15: Recovery of motor units responsible for generating 15%MVC in the SPiTFiRe model 32

Figure 16. Bertec PY6 force transducer with attachment plates, showing the force axes (X,Y,Z) and a potential point of application of the force (F) (Bertec Corporation, 2012) ... 35

Figure 17. Participant setup for triceps contraction protocol. 36

Figure 18. EMG Trigno mini sensor 36

Figure 19: Grass S48 Muscle Electrical Stimulator 38

Figure 20: Axelgaard PALS® electrodes 39

Figure 21. Flowchart of protocol elements 41

Figure 22. Raw force response from 100 Hz (left) and 20 Hz(right) triceps stimulations ... 42

Figure 23: An outline of the windowing of force using EMG response from the long and lateral heads of the triceps 45

Figure 24: Average MVF outputs stratified by intensity (high versus low) and time (pre versus post) 49

Figure 25: NFRs during recovery following completion of the high and low intensity fatigue protocols (collapsed across stimulation frequency). The vertical dashed line represents the baseline force response for reference. '*' = Significantly different pairwise comparison between intensities specific to each time point. 51

Figure 26: NFRs measured at high and low frequency stimulations during recovery (collapsed across intensity). The vertical dashed line represents the baseline force response for reference. '*' = Significantly different pairwise comparison..... 52

Figure 27: Average percent activation of triceps brachii and biceps brachii during high intensity protocol across all participants 53

Figure 28: Average percent activation of triceps brachii and biceps brachii during low intensity protocol across all participants 54

Figure 29: Comparisons between the overall muscle stimulation-measured recovery and SPiTFiRe-simulated recovery from fatigue accumulation following 20%MVF and 70%MVF protocols, normalized to baseline. 58

Figure 30: Absolute mean force responses from 100 Hz and 20 Hz stimulation frequencies across high and low intensities..... 71

Figure 31: Normalized mean force responses from 100 Hz and 20 Hz stimulation frequencies across high and low intensities 72

List of Tables

Table 1: Summary of participant demographics. 34

Table 2. Delsys Trigno mini specifications 37

Table 3. Electrode location and orientation based on the muscle of interest 37

Table 4: Settings for Muscle Stimulation Unit and Isolation Unit 40

Table 5: Descriptive statistics for maximum voluntary force, stimulation voltage, and endurance time stratified by protocol. 48

Table 6: Results from the Three-Way Repeated Measures Analysis of Variance 50

Table 7: Results from the pairwise comparisons of normalized force responses at high and low intensities to baseline across time 73

Table 8: Results of the pairwise comparisons of normalized force responses between high and low intensities across time 73

Table 9: Results from the pairwise comparisons of normalized force responses at high and low frequencies to baseline across time 75

Table 10: Results of the pairwise comparisons of normalized force between high and low frequencies across time 76

Table 11: Average Normalized Force Response following the low intensity (20%MVF) and high intensity (70%MVF) protocols 77

Table 12: Average percent activation of the long and lateral heads of the triceps brachii, and of the biceps brachii, during the high intensity protocol (70%MVF) 78

Table 13: Average percent activation of the long and lateral heads of the triceps brachii, and of the biceps brachii, during the low intensity protocol (20%MVF) 79

List of Equations

Equation 1 shows the distribution of motor units based on the desired range of twitch forces (RP) across the motor unit pool based on each motor unit (i), and n is the number of motor units in the pool (12) (Fuglevand et al., 1993; Potvin and Fuglevand, 2017a) 24

Equation 2 represents the threshold level of excitation for each motor unit, where RTE is the recruitment threshold excitation, RR is the desired range of recruitment thresholds, and n is the number of motor units. 24

Equation 3 represents the nominal fatigue rate associated with the contraction type (FAT), and RFR represents the range of fatigabilities across the motor unit population. 25

Equation 4 shows the equation used to calculate the rate of recovery (Potvin & Fuglevand, 2018) of a given motor unit, where A(t,E) represents the intrinsic adaptation current, itself dependent on the length of time the motor unit has been recruited (t) and the excitation level (E). 25

Equation 5 represents the calculation of a participant's average percent activation at a given time window based on the average EMG amplitude during that window (i), and the average maximum EMG amplitude obtained from the MVC trial. 46

1.0 Introduction

Continuous exposure to physical hazards in the workplace can lead to the development of musculoskeletal disorders (MSDs). As of 2014, the annual estimate to treat and manage chronic pain was up to $7.2 billion for Canadian workers (Hogan et al., 2016). This type of pain and injury can be disabling and pervasive, progressively decreasing quality of life with age (Briggs et al., 2016). While there may be many mechanisms of injury progression, chronic MSDs resulting from fatigue, a large portion of which are muscular in nature, result in $300 million in annual losses in the United States alone (Cavuoto, 2016). However, practitioners have limited access to tools to assess and control potentially fatiguing exposures in the workplace (Enoka & Duchateau, 2016). This is despite evidence suggesting that muscle fatigue-related changes can be responsible for direct damage through metabolite accumulation (Visser & Van Dieën, 2006), and indirectly through the compensatory alteration of movement kinematics (Côté, 2014; Côté et al., 2002). Fatigue accumulation is also influenced by the variability of the jobs themselves; work tasks may require the generation of any combination of static and/ or dynamic contractions, all of which may influence the exposure on the body, subsequent fatigue accumulation, and injury risk (Gallagher & Schall, 2017; Mehdizadeh et al., 2020). Additionally, understanding the recovery needs of the worker in between periods of fatiguing work could allow practitioners to extend their knowledge of fatigue accumulation and recovery across multiple tasks, work shifts, and workdays.

Muscle force-time requirements influence fatigue and recovery. Mathematical models have attempted to define the relationship between muscle force-time requirements and fatigue and recovery. Models that can provide more objective information about whether a designed job is

providing sufficient muscle recovery between tasks could be incorporated into workplace ergonomics assessment tools, but first require validation to justify their use. However, existing models of muscle fatigue and recovery that consider complex force-time histories are few (Frey-Law et al., 2021; Potvin and Fuglevand, 2018), and require validation of their in-silico assumptions. In particular, Potvin & Fuglevand (2018) proposed the Size Principle Transient Fatigue and Recovery (SPiTFiRe) model, which attempts to predict muscle motor unit fatigue and recovery based on the time-series intensity of muscle force required. The model predicts the fatigue and recovery rates for each motor unit within a pool of 120 motor units based on the assumption that a greater proportion of slow twitch, fatigue-resistant motor units are active to complete tasks requiring low forces over a prolonged time period, and subsequently require a longer recovery time (Potvin and Fuglevand, 2018, 2017a). In contrast, high-force generating, but fatigable, fast twitch motor units were modelled to be active at greater force intensities, and fatigue and recover faster than the slow twitch motor units (Potvin and Fuglevand, 2018, 2017a). While previous literature supports the relationship between force intensity and motor unit recruitment and fatigue (Fuglevand et al., 1993; Henneman et al., 1965; Jones, 1996; Visser & Van Dieën, 2006; Vøllestad, 1997), less experimental evidence is available about recovery. It is necessary to validate the model's prediction of the decline in muscle pooled motor unit capacity to assess whether the time to recovery is dependent on the distribution of fatigue between slow- and fast- twitch motor units. Observing how human participants recover from muscle fatigue may help us better understand the relationship between fatigue and recovery, a next step towards integrating fatigue and recovery predictions into workplace ergonomics assessment tools.

The purpose of this thesis was to test the hypothesis that recovery from motor unit fatigue accumulation differed when the triceps brachii were fatigued using task intensities that

preferentially targeted larger motor units, relative to task intensities that additionally targeted smaller motor units. By investigating this thesis, I provide empirical validation for the hypothesis that recovery is dependent on the type of motor unit fatigued, an important current assumption underpinning the use of the SPiTFiRe model. Addressing the gap between key descriptors of muscle fatigue and recovery can help evolve existing mathematical models into field-ready ergonomics assessment tools that are able to quantify the risk associated with multitask fatigue accumulation in the workplace.

Research Question: Does the normalized muscle force response measured at the triceps brachii at prescribed post endurance time intervals using high (100Hz) and low (20Hz) frequency electrical stimulations differ between fatigue accumulation caused by the performance of sustained high (70% of their Maximum Voluntary Force (MVF)) versus low (20%MVF) intensity isometric elbow extensions among a sample of healthy, right-handed participants?

Hypothesis 1: The normalized muscle force response at each time point will be greater following the high intensity protocol compared to the low intensity protocol, indicating that recovery from fatigue following high intensity work is faster.

Hypothesis 2: The normalized muscle force response at each time point will be greater following the 100Hz stimulation compared to the 20Hz stimulation, indicating that larger motor units recover faster than smaller motor units.

2.0 Literature Review

2.1 Integration of muscle fatigue models towards ergonomics assessments

While a single high intensity physical exposure can push beyond the capacity of a worker and cause injury, MSDs likely occur more often from sustained exposure to lower intensity tasks (Jones, 1996). However, hazard exposure assessment tools have typically focussed on single task exposures (Lowe et al., 2019; Mehdizadeh et al., 2020). Therefore, while both pathways might lead to the development of MSDs the actual level of MSD hazard exposure accumulation for an entire work shift (or longer) may not be adequately quantified, and therefore resultant interventions may not effectively reduce workplace injury incidence (Jones & Kumar, 2010). I conducted a scoping review to identify hazard exposure assessment tools capable of assessing accumulated exposures, and learned that tissue level exposures were expressed as being related to either mechanical loading or muscle fatigue accumulation, but few user-ready tools existed to quantify exposures related to the accumulation of muscle fatigue (Figure 1) (Veerasammy et al., 2022).

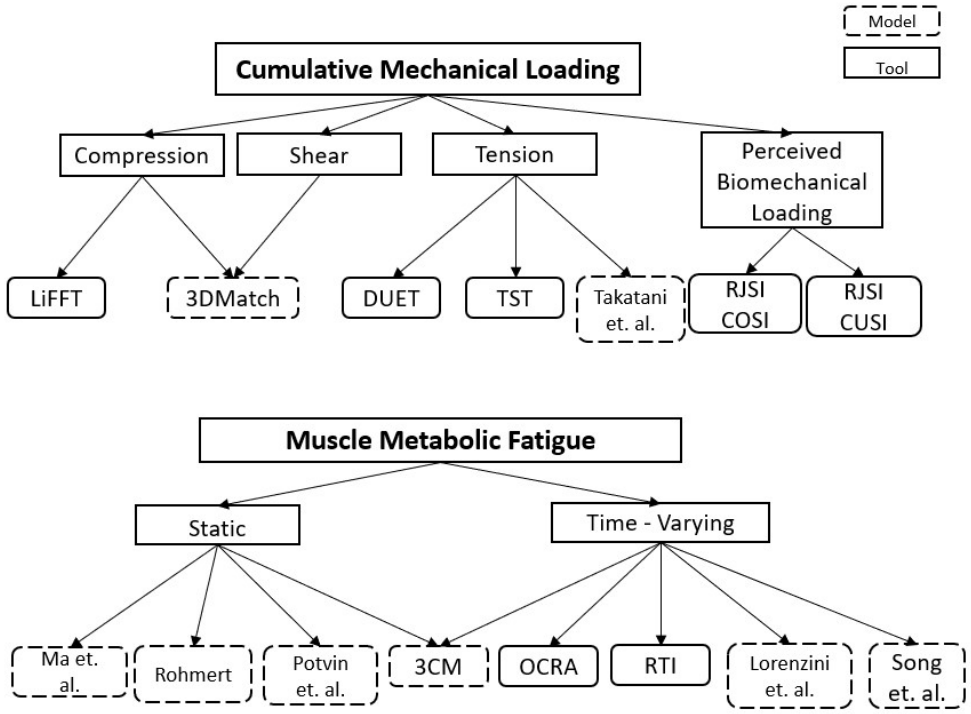

Figure 1. Summary of tools and models addressing either Cumulative Mechanical Loading or Muscle Metabolic Fatigue based on their internal tissue mechanism of loading.

Workers may still be pathologically fatigued if rest requirements are not considered in workplace designs. While the concept of rest emerged as an important criterion to properly inform job organization, a lack of muscle fatigue assessment tools, as well as a limited ability to estimate recovery requirements when fatigue exists, may cause ergonomists to underestimate cumulative work exposure risk (Mehdizadeh et al., 2020; Neumann et al., 2020; Takatani and Bruchal, 2017). A lack of sufficient muscle recovery through breaks within and between shifts could result in chronic pain and injury, either through direct damage to muscle fibers (Allen et al., 2008; Fitts, 2021; Visser and Van Dieën, 2006) or indirectly through inappropriate kinematic compensations (Côté et al., 2002; Gates and Dingwell, 2008; Kumar, 2001)

A worker's ability to generate force depends on the state of fatigue and recovery within the muscles activated to perform a task. Quantifying and integrating information about the relationships between a worker's external force generation, muscle activation, fatigue

accumulation and recovery patterns into tools and wearable technologies may strengthen the ability to capture fatigue-related drivers of WMSDs (Wells et al., 2004). Increased utility of these tools can also be possible through the incorporation of readily accessible inputs into fatigue models (such as repetition, duration, or posture) (Chiang et al., 2008; Dempsey et al., 2018). Addressing the lack of literature connecting muscle metabolic fatigue to workplace injury incidence can better inform the risk associated with multitask fatigue accumulation across varying rest allowance levels (Neumann et al., 2020). In doing this, ergonomics injury risk assessment tools can then provide a justifiably causal link between occupational exposures and the probability of an injury outcome.

2.2 Muscle Motor Unit Properties and Activation

2.2.1 Skeletal Muscle Properties

Skeletal muscles are the force producing components of the body. When muscles contract and shorten, they act at joints to create movement and/ or maintain position. This process is said to occur within sarcomeres, the active contractile unit within muscles (Frontera and Ochala, 2015). Within the sarcomere, the shortening of these fibers have been proposed to occur as a result of the sliding of the thick and thin filaments over each other (Huxley and Niedergerke, 1954) in an energy dependent process (Figure 2).

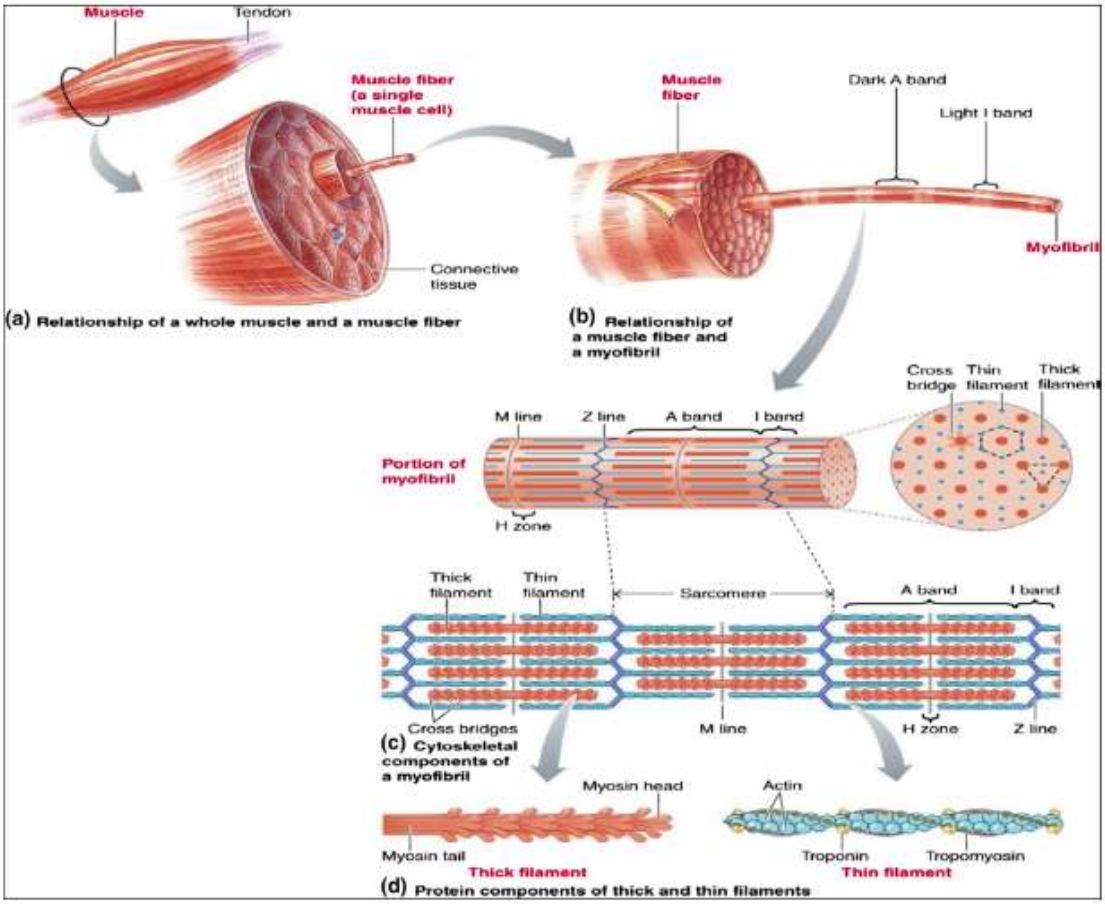

Figure 2. Skeletal muscle properties (Frontera and Ochala, 2015).

Muscle fibers can vary in their force generating capacity and fatigue resistance. This is mainly based on their sarcomere shortening speed and their preferential use of oxidative versus glycolytic pathways (Frontera and Ochala, 2015). Slow twitch, oxidative (Type I) fibers are considered fatigue resistant while fast twitch, glycolytic (Type II) fibers are considered fatigable, but generate larger forces as a result of having more muscle fibers with relatively larger cross-sectional areas.

2.2.2 Motor Unit Properties and Force Generation

A motor unit is the connection between the signals sent by the peripheral nervous system through a somatic motoneuron, and the force generating muscle fibers it innervates (Henneman et al., 1965; Hof, 1984). Each motoneuron is connected to the muscle fibers through a synapse with the motor endplate (Hof, 1984) (Figure 3).

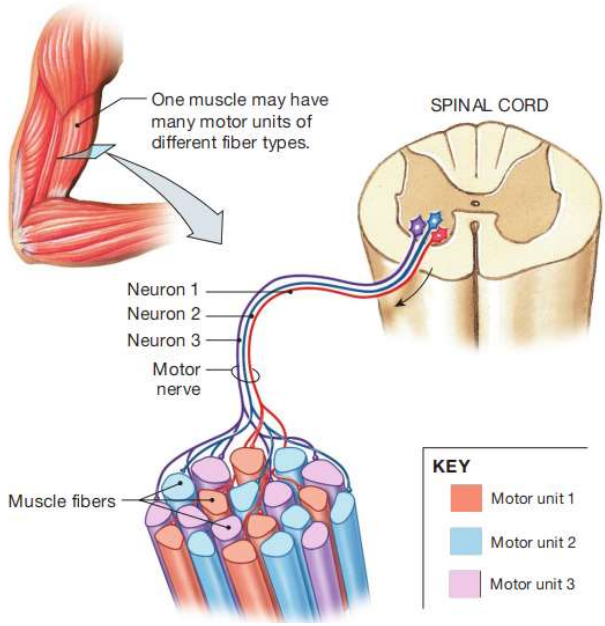

Figure 3. The arrangement of motor units. Groups of somatic motor neurons extend from the spinal cord and synapse onto a group of muscle fibers (Silverthorn, 2007).

Activation of muscle fibers in motor units occurs through Excitation-Contraction coupling. Stimulation of the somatic motor neuron triggers the release of Acetylcholine (Ach) at the neuromuscular junction of the muscle fiber (Lymn and Taylor, 1971). This triggers the release of sodium (Na+) ions through the receptor channels, creating a muscle action potential. This action potential culminates in the downstream release of calcium (Ca2+) ions from the sarcoplasmic reticulum (SR) into the cytoplasm. The Ca2+ ions bind to troponin and initiate the

cross bridge cycle after the hydrolysis of the ATP molecule on the myosin molecule provides energy for it to attach to actin (Lymn and Taylor, 1971). The collective formation of these cross bridges generates the muscle force required to meet external task demands. Sustaining these skeletal muscle contractions require a constant supply of potassium (K+) ions, which work in tandem with Na+ ions to pump Ca2+ back into the SR during the relaxation phase using ATP (Fowles et al., 2002).

Muscle force generation is coordinated through a combination of motor unit activation (recruitment) and increasing the firing rate of the active units (rate coding) (Hof, 1984). Henneman's size principle dictates that recruitment of motor units occurs in order of size, with the smallest motor units being recruited first, and an increase in motor unit recruitment based on size in a graded response to higher force demands (Henneman et al., 1965) (Figure 4). For example, low intensity efforts may result in the prolonged activation of predominantly smaller fatigue-resistant motor units, with minimal activation of larger, more fatigable motor units (Fuglevand et al., 1993; Hof, 1984; Potvin and Fuglevand, 2017a). However, while increasing force demands over short bursts of activity would result in a greater activation of larger, more powerful, fast twitch motor units, slow twitch motor units would still be activated first, irrespective of force magnitude (Fuglevand et al., 1993; Henneman, 1957; Hof, 1984; Potvin & Fuglevand, 2017).

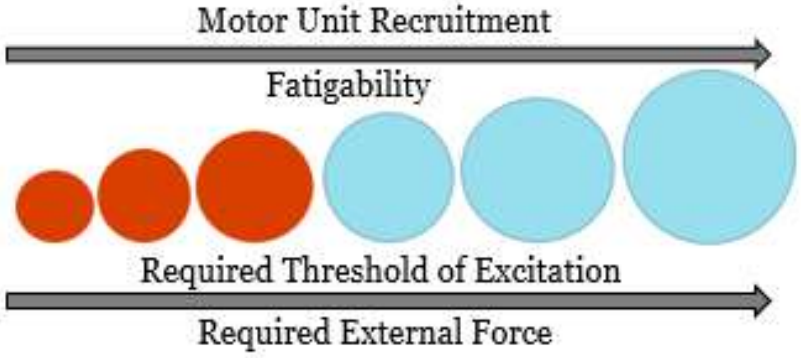

Figure 4. The increasing motor unit size increases their threshold of excitation, force generating capacity, and fatigability

2.2.3 Motor Unit Fatigue

Muscle fatigue can be described in many different ways, but all relate in that they describe some form of performance decline. This decline can be measured over a discrete time period, due to the inability of a muscle or a group of muscles to sustain the required force (Bigland-Ritchie and Woods, 1984; Enoka and Duchateau, 2016). Fatigue can even be classified as the decline in the maximum force generating capacity, regardless of whether the target force is being met (Bigland-Ritchie and Woods, 1984). Fatigue can occur through any combination of central and/ or peripheral mechanisms (Bigland Ritchie et al., 1978; Binder-Macleod and Russ, 1999). Peripheral fatigue mechanisms can affect the motor unit through electrochemical impairments that impair the mechanical force generating ability of cross bridges. Central fatigue mechanisms may impair voluntary contractions through a reduction in the neural input sent by the central nervous system to activate motor units (Bigland Ritchie et al., 1978; Binder-Macleod and Russ, 1999). Both central and peripheral impairments of motor units result in the decline in the muscle force generating capacity, indicative of fatigue (Enoka and Duchateau, 2008; Fuglevand et al., 1993).

The dominant mechanism of fatigue (central or peripheral) may depend on the intensity of task being performed, the participant's motivations, and the type of muscle being fatigued (Bigland Ritchie et al., 1978). Central fatigue may result in the rapid decline in muscle force and tends to be associated with maintaining high intensity contractions (Allen et al., 2008). In contrast, peripheral fatigue has been associated with failure in the contractile apparatus of the motor units and is associated with the prolonged performance of low intensity contractions (Allen et al., 2008). Regardless, both central (ratings of perceived exertion) and peripheral (electromyography, muscle stimulation) measures of fatigue must be considered to better understand task failure mechanisms (Yung and Wells, 2017).

Specific to peripheral fatigue mechanisms, Section 2.2.2 outlined the processes through which a motor unit generates the task required force, including the ions required for this to occur. Limitations to any point of these processes can lead to the inability to generate the required force, indicating the onset of fatigue (Figure 5).

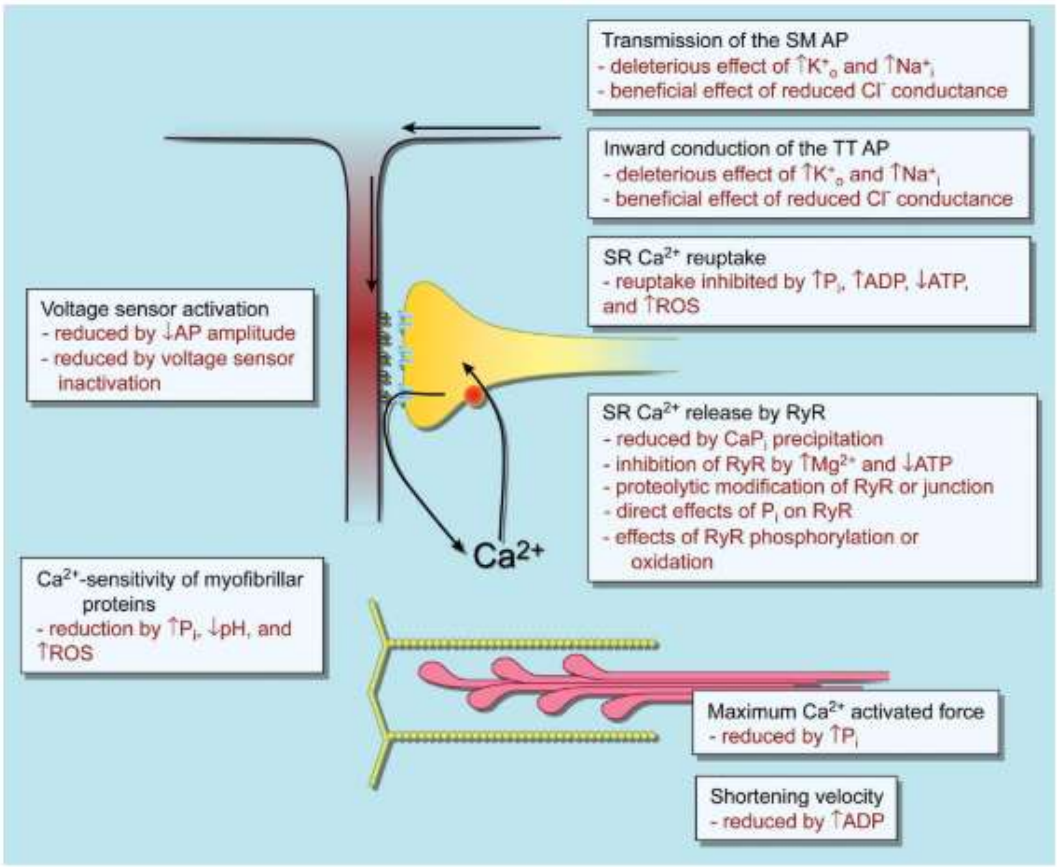

Figure 5. Mechanisms of Peripheral Fatigue (Allen et al, 2008)

Increased concentrations of inorganic phosphate (Pi) through the ATP dependent reactions in the cross bridge contraction and relaxation cycles reduces force production, Ca^{2+} release from the SR, and sensitivity of Troponin to Ca^{2+} binding (Allen et al., 2008; Fitts, 1994). This increased concentration is responsible for the decrease in force production in larger motor units (Allen et al., 2008). Additionally, with high intensity efforts, the rapid depletion of ATP results in the reduced rate of Ca^{2+} release into the cytoplasm and therefore reduces the rate of troponin binding (Allen et al., 2008). In contrast, with prolonged, exhausting exercise, depletion in glycogen (a core energy provider) results in the decrease in SR Ca^{2+} release (Allen et al., 2008). It is also important to consider that an individual is able to maintain low intensity efforts much longer than high intensity efforts. However, while metabolites may likely accumulate for a

longer duration during a lower intensity effort, there is a greater rate of metabolite accumulation during a higher intensity effort (Suga et al., 2012). Therefore, while a greater buildup of metabolites would impair a motor unit's force generating ability as a function of time, it is unclear whether this buildup will be greater as a result of a longer duration low intensity effort or a shorter duration high intensity effort .The eventual task failure as a result of the greater overall fatigue accumulation could result in a more physiologically demanding effort to remove metabolites, and therefore would result in a longer time for the fatigued muscle to recover its full maximal force generating capacity.

The onset of muscle fatigue is indicated by the impairment in the ability of the muscle to generate the required force. This phenomenon could potentially be mapped in order to predict fatigue onset and recovery times based on task requirements. However, accurate prediction of motor unit activation, fatigue, and recovery requires consideration of differences based on motor unit size, force generating capacity, fatigability, and firing rate (Henneman et al., 1965; Rashedi and Nussbaum, 2016).

2.2.5 Motor Unit Fatigue Recovery

A worker can recover from fatigue accumulation during task performance (Yung, 2016) , between tasks (Gallagher et al., 2017), and between work shifts (Cavuoto, 2016; Yung et al., 2014). The required recovery time, however, may differ with regards to the preferential activation of fast or slow twitch motor units. Fast twitch motor units, once activated, remain activated for a shorter period compared to slow twitch motor units (Kernell & Monster, 1982; Visser & Van Dieën, 2006). This can be seen in the performance of high intensity tasks, where workers may only be able to perform for a short period, taking more frequent breaks. In contrast, slow twitch motor units would have greater metabolite accumulation, and would require greater

recovery time following fatigue (Fuglevand et al., 1993; Jones, 1996; Potvin & Fuglevand, 2017). Prolonged, low intensity efforts may therefore result in fatigue that takes longer to manifest, but creates recovery demands that carry over to subsequent- work-days (Cavuoto, 2016; Yung et al., 2014).

2.3 Measuring Muscle Fatigue and Recovery

The lack of validated experimental models of muscle fatigue and recovery has made it difficult to accurately assess worker fatigue and recovery in the field (Enoka & Duchateau, 2016). More robust models of muscle fatigue and recovery measurements will lead to designing ergonomics assessment tools that are more accurate quantifiers of muscle fatigue and injury risk, while simultaneously making cutting edge research accessible to ergonomists (Shorrock and Williams, 2016). Currently, EMG measurements are used in laboratory settings to track fatigue development, and muscle stimulation has been used as a means of tracking motor unit recovery (Yung et al., 2012). With regards to modelling these relationships, the Size Principle Transient Fatigue and Recovery (SPiTFiRe) model (Potvin and Fuglevand, 2018) proposes that muscle fatigue and recovery is dependent on the force time history of muscle activation, where a much greater recovery time is expected for tasks resulting in fatigue through low force/high duration contractions when compared to those that result in fatigue from high force/ short duration tasks.

2.3.1 Surface Electromyography

Surface Electromyography (EMG) tracks the electrical behaviour of target muscles during a task. Surface EMG can be used to track the onset of neuromuscular fatigue, where the ability of motor units to voluntarily generate muscle force is impaired (Bigland-Ritchie, 1981). During the performance of a task, constantly trying to maintain a target force results in the

gradual fatigue and drop-off the currently recruited motor units (Visser and Van Dieën, 2006). To maintain the target force, larger motor units will be recruited, which is seen as an increase in EMG magnitude in the time domain (Bigland-Ritchie, 1981) (Figure 6). When the largest force generating motor units are unable to generate the target force, there is a subsequent drop-off in both force and EMG activity (Bigland-Ritchie, 1981).

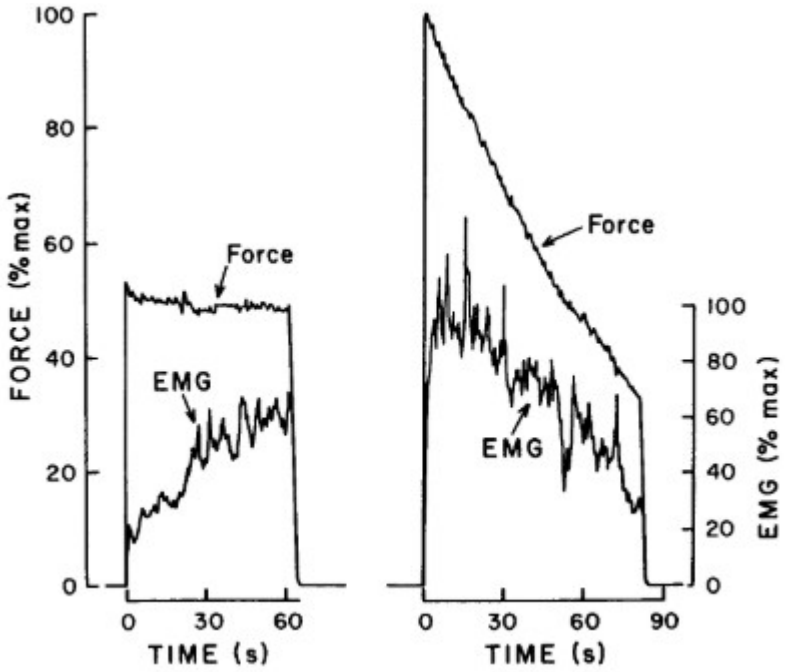

Figure 6. Diagram displaying the increase in muscle EMG activity to maintain a prolonged target force(left) and the subsequent drop-off when the target force cannot be sustained by the largest motor units (right) (Bigland-Ritchie, 1981).

With regards to the constant engagement of slow twitch motor units, it was found that fewer "gaps" in surface EMG recordings (<0.5%MVC) were closely associated with greater pain complaints (Hägg and Åström, 1997; Veiersted et al., 1990). This was further proposed to be due to the impairment of the excitation-contraction coupling process, where the depletion of cytosolic Ca^{2+} needed to bind to troponin to initiate the cross bridge cycle caused a reduction in

the slow twitch motor unit's ability to maintain muscle tension (Adamo et al., 2009; Vøllestad, 1997). However, the EMG shift towards lower frequencies with fatigue from performance of a high intensity task may not be seen with fatigue from low intensity task performance (Moxham et al., 1982). Therefore, other measures, such as muscle electrical stimulation, may be required to assess the extent of low intensity muscle fatigue and recovery (Yung and Wells, 2017).

2.3.2 Muscle Electrical Stimulation

Measures of Maximum Voluntary Force (MVF) generated through a Maximum Voluntary Contraction (MVC) from a participant's muscles have been used to assess whether the targeted muscles had fully recovered their force generating capacity following a fatigue protocol (Vøllestad, 1997). However, this may not provide information on the state of slow twitch motor units, as the assessment itself preferentially fatigues larger, fast twitch motor units (Jones, 1996; Vøllestad, 1997). Figure 8 uses the SPiTFiRe model (see section 2.3.3) to demonstrate the behaviour of a group of motor units of increasing size (from top to bottom) during a 10-second simulated MVC, as well as three minutes of recovery. Each motor unit is colour coded. The red lines represent the smallest motor units, lighter shades of red, orange, and yellow represent larger motor units, while increasing shades of blue represent the largest motor units in the pool. The black line represents the collective decline and recovery of the pool's force generating capacity.

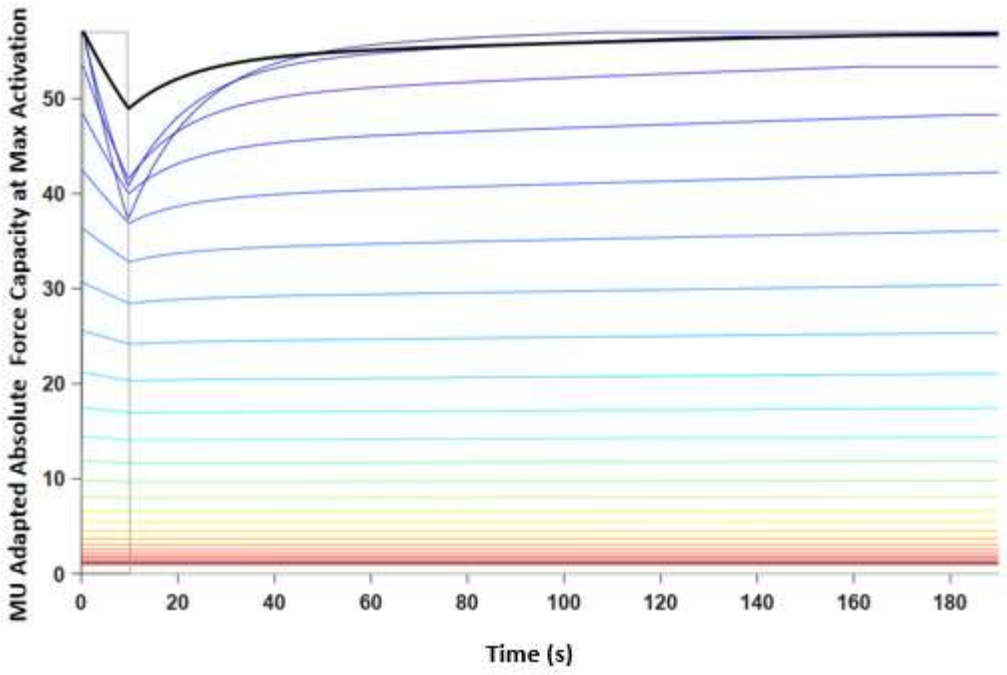

Figure 7. Assessing level of recovery through an MVF preferentially assesses the fatigue and recovery of larger motor units, as illustrated using the SPiTFiRe.

The decline in force production shown here is driven by the drop in capacity of the largest motor units, while the smallest motor units remain relatively unfatigued (Potvin and Fuglevand, 2017a). Similarly, recovery of the muscle's force generating capacity is driven primarily by that of the largest motor units in the pool (Potvin and Fuglevand, 2018). Therefore, measures of recovery should also target the recovery rates of small motor units.

Measuring muscle tetanic force through electrical stimulation may be effective in assessing smaller motor units (Hales and Gandevia, 1988; Vøllestad, 1997). Stimulation uses the muscle's rate coding relationship i.e. the relationship between the electrical input from the muscle's somatic motor neuron to the motor endplate that triggers a muscle contraction (Enoka, 2019). An electrical stimulus would be delivered at the nerve during a submaximal voluntary

contraction (voluntary tension), and this allows the muscle to increase its contractile force equal to the additional motor units that are stimulated to form cross bridges (tetanic tension) that generates a twitch force response (Shield and Zhou, 2004; Vøllestad, 1997). The relationship between the electrical stimulation administered and the resulting tetanic tension/ twitch force response can be compared between the muscle's unfatigued state and at different time points following fatigue as a measure of recovery (Figure 9) (Vøllestad, 1997).

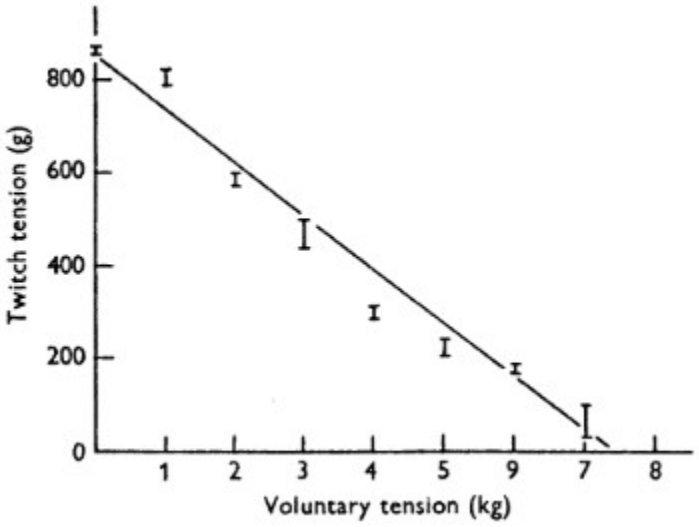

Figure 8. Typical relationship between voluntary tension and tetanic tension to assess reserve capacity of thumb adductor; the greater the voluntary tension, the lower the contribution from the tetanic tension (Vøllestad, 1997).

By electrically stimulating an unfatigued muscle, a fatigued muscle, and a muscle that is recovering, we may learn more about fatigue and recovery processes. However, the type of knowledge that can be gained depends on the amplitude and frequency of the electrical stimulation (Figure 10).

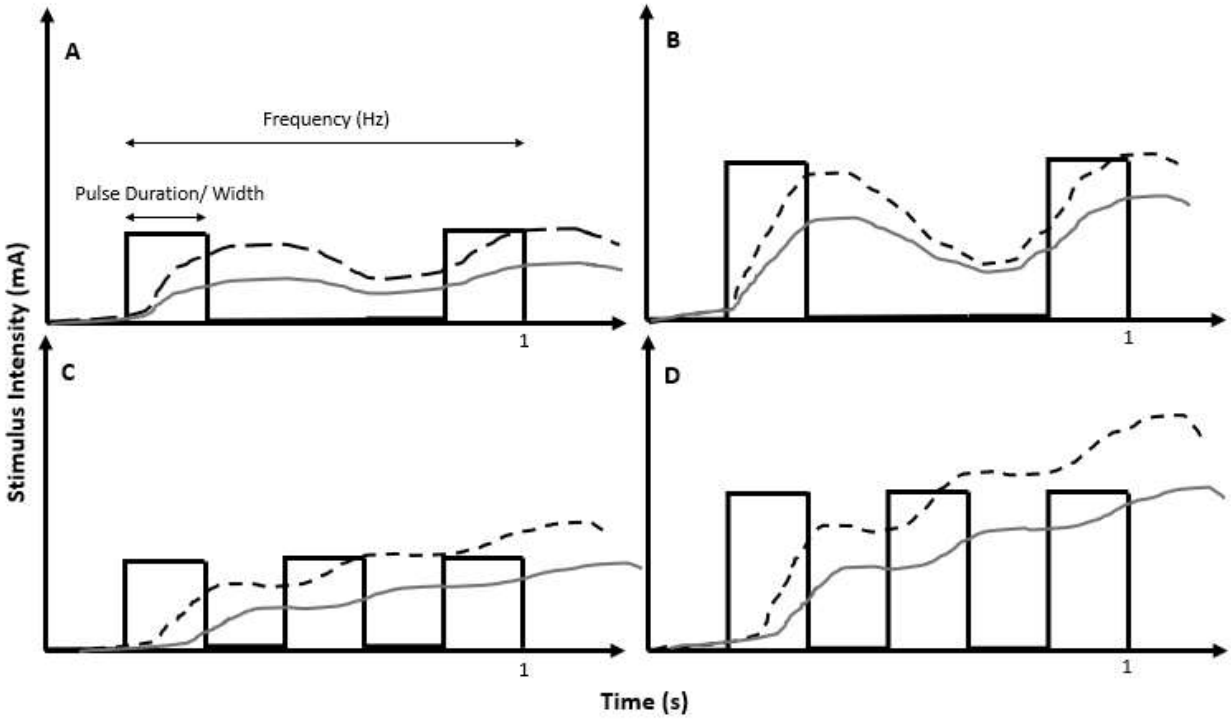

Figure 9. Visualization of how changing the stimulus intensity (mA) and frequency (Hz) from a muscle stimulator changes the intensity of muscle contractions (%MVC), represented by the dotted black (unfatigued) and solid grey (fatigued) lines.

Figure 9A illustrates a typical, baseline, 2Hz input from a muscle stimulator. This input may change as a function of intensity (Figure 9B), pulse frequency (Figure 9C), or both (9D), which influences the extent of motor unit recruitment, and therefore the intensity of muscle contraction elicited (Adamo et al., 2009; McKenzie et al., 1992). In particular, increasing the frequency of electrical stimulation increases the extent of fused tetanic contractions through meeting the activation threshold of the largest motor units (Adamo et al., 2009; Henneman, 1957). Additionally, as muscles fatigue, their response to these electrical stimulations will be diminished. By assessing the extent of this decline across high and low frequency stimulations, an understanding of the level of fatigue and recovery can be established (Adamo et al., 2009;

Dennerlein et al., 2003; Yung et al., 2012). Specifically, there may be more rapid force recovery from high frequency stimulation (such as 100Hz) driven by the largest motor units, compared to low frequency stimulation (such as 20Hz), limited by the smallest motor units (Dennerlein et al., 2003; Yung, 2016). Figure 10 visualizes the muscle force response from a held force transducer that would be expected if the muscle was stimulated at high (100Hz) and low (20Hz) frequencies.

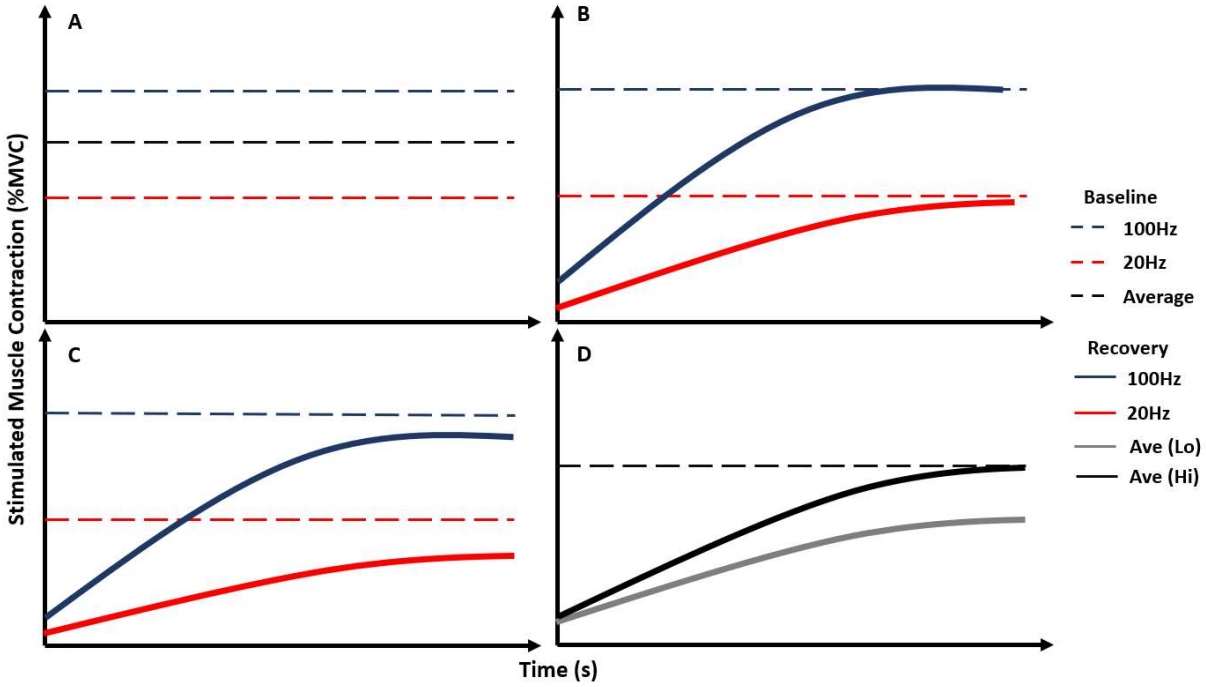

Figure 10. Simulated muscle force response at baseline (A) and recovery following fatigue at high (B) and low (C) intensities. The muscle would have been electrically stimulated at high (100Hz) and low (20Hz) frequencies, and the average expected to be found (D).

The blue lines represent stimulation at 100 Hz, while the red lines represent stimulation at 20Hz that follows. At baseline (pre-fatigue) (10A), the force output from stimulation would be constant at both frequencies, though the 100Hz frequency would elicit a greater force. The black line represents the average force response which would also remain constant at baseline.

However, at different time points following recovery from fatigue occurring due to either high (10B) or low (10C) intensity work, initial stimulations would elicit a lower force response at both frequencies, though the average normalized force response (NFR) across protocols would be much more diminished and take longer to recover following fatigue from the low intensity task compared to the high intensity task (10D).

Muscle electrical stimulation can be used to assess how efficiently the muscle is able to generate a muscle contraction under high- and low- frequency stimulations (Yung et al., 2012), which is further indicative of the extent under which cytosolic Ca^{2+} is still available to bind to troponin (Figure 11) (Vøllestad, 1997). Figure 11 also outlines the overlap between muscle stimulation and MVC to identify cytosolic mechanisms of fatigue, where muscle stimulation (Tetanic force) provides a greater sensitivity to the detection of fatigue and recovery in smaller motor units.

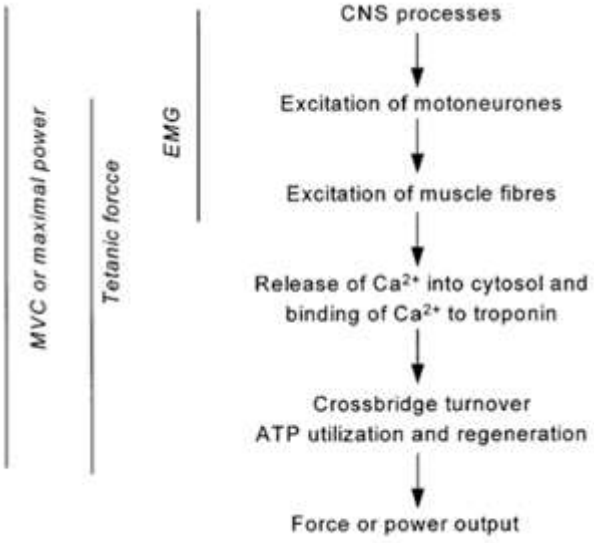

Figure 11. The overlap between EMG, evoked tetanic force through muscle stimulation, MVC, and the underlying neuromechanical processes resulting in muscle fatigue.. EMG: Electromyography; MVC: Maximum Voluntary Contraction (adapted from Vøllestad, 1997).

There is a direct relationship between the level of muscle fatigue, and a muscle motor unit's sensitivity to electrically stimulated tetanic force generation (Bigland-Ritchie and Woods, 1984; Vøllestad, 1997; Yung et al., 2012). Additionally, researchers have demonstrated the decline in muscle tetanic force response to low frequencies versus high frequencies as indicative of low frequency fatigue (Adamo et al., 2009; Yung et al., 2012). However, it is uncertain if this implies that the driver of this relationship is the fatigue and recovery of smaller versus larger motor units. It may be that fatigue as the result of the prolonged performance of low intensity contractions may result in greater decline in force generating capacity of both smaller and larger motor units. Therefore, recovery from a low intensity task may result in a lower recovery slope when compared to recovery from the same task being performed at a higher intensity, due the slower recovery time in smaller motor units.

It was assumed that high frequency electrical stimulations were more likely to recruit the larger motor units, and low frequency stimulation will recruit the smaller motor units, in accordance with Henneman's size principle (Henneman, 1957). However, previous research has also proposed that motor unit recruitment may occur as a result of an inverse size principle (Hamada et al., 2004), where an electrical stimulation is said to preferentially recruit the largest motor units first. Others have proposed that muscle fiber recruitment as a result of electrical stimulation may be random and non-selective (Gregory and Bickel, 2005). The potential for these phenomena to occur was considered when muscle electrical stimulation was used as a measure of motor unit recovery.

2.3.3 The SPiTFiRe Model

The SPiTFiRe model is based on previous work done by Fuglevand et. al. (1993), which attempted to model recruitment and rate coding of motor units based on a signal from the central nervous system to the motor neuron, and the action potentials that signal the activation of motor units of increasing size. The current model proposes the activation, fatigue and recovery of motor units when meeting muscular demands (Potvin and Fuglevand, 2018), and is outlined in Figure 12.

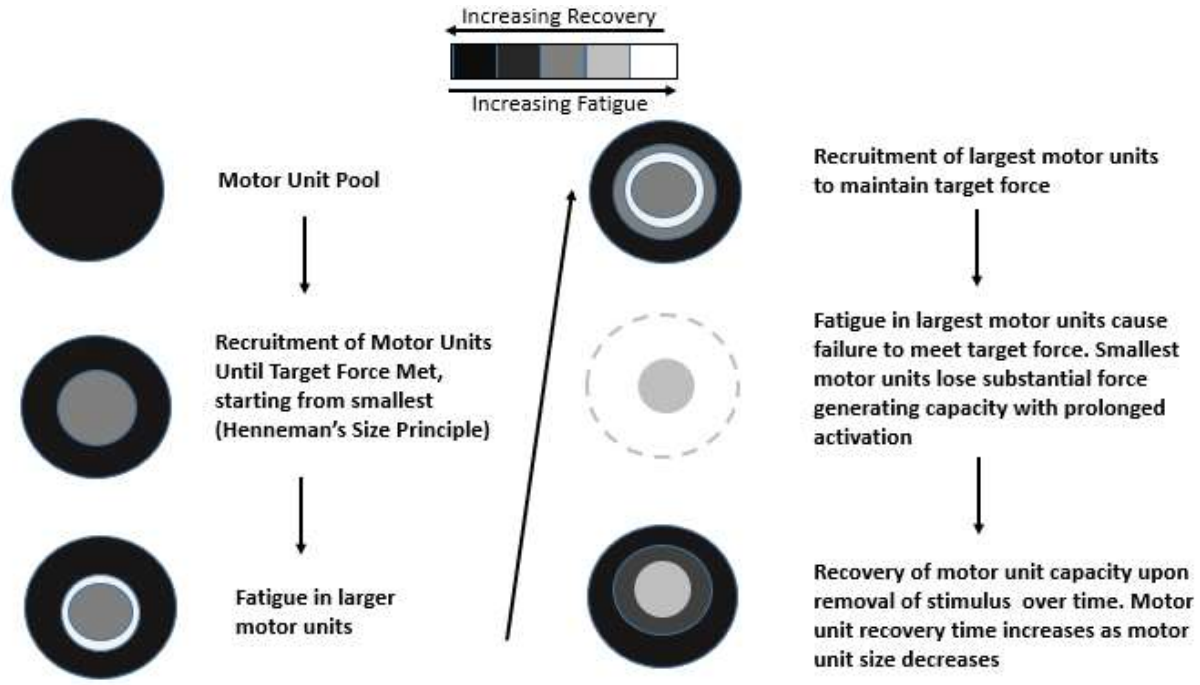

Figure 12. Flowchart of SPiTFiRe model processing

In Figure 12, the inner circle represents the smaller motor units, which are activated in accordance with Henneman's size principle (Henneman, 1957). That circle grows, representing the increasing number of motor units recruited to meet the target force requirements. But larger motor units tend to fatigue more rapidly, such that the largest active motor units (outer edge of

the grey circle) may begin to fatigue (white ring). To accommodate for the fatigue, higher threshold motor units are recruited (grey circle grows). This process of recruitment and fatigue continues until either the task is completed, or the largest motor units experience a loss in force generating capacity that renders them unable to meet the target force. Upon removal of the stimulus, the motor units begin to recover, with the largest motor units requiring the shortest time to reach full recovery and the smallest motor units requiring the longest time to recover.

The motor unit pool is distributed such that there are a higher proportion of slow twitch, fatigue-resistant muscle fibers, and relatively fewer fast twitch, fatigable muscle fibers (Fuglevand et al., 1993; Potvin and Fuglevand, 2017a), as distributed by Equation 1 below.

$$P(i) = e^{[\frac{\ln(RP)(i-1)}{n-1}]}$$

Equation 1 shows the distribution of motor units based on the desired range of twitch forces (RP) across the motor unit pool based on each motor unit (i), and n is the number of motor units in the pool (12) (Fuglevand et al., 1993; Potvin and Fuglevand, 2017a)

Potvin & Fuglevand (2017) used this underlying model to predict muscle fatigue for a series of isometric contractions. First, the minimum threshold of excitation for each motor unit was established, as per Equation 2 below (Potvin and Fuglevand, 2017a).

$$RTE(i) = e^{[\frac{\ln(RR)(i-1)}{n-1}]}$$

Equation 2 represents the threshold level of excitation for each motor unit, where RTE is the recruitment threshold excitation, RR is the desired range of recruitment thresholds, and n is the number of motor units.

The motor units that meet the threshold level of recruitment, were activated and contributed to the overall muscle firing rate and force output (Potvin and Fuglevand, 2017a), and eventually fatigued as per Equation 3 below.

$$FAT(i) = FAT(1)x\ e^{[\frac{\ln(RFR)(i-1)}{n-1}]}$$

Equation 3 represents the nominal fatigue rate associated with the contraction type (FAT), and RFR represents the range of fatigabilities across the motor unit population.

The recovery from this fatigue was modelled by Potvin & Fuglevand (2018) in the most recent iteration of the model. The rate of recovery was modelled such that the faster the motor unit's adaptation to recruitment, which corresponds to the larger the force contribution, the faster the recovery will be. This ensures that the slow twitch, fatigue-resistant motor units recover at a slower rate from continuous activation, while the fast twitch, fatigable motor units recover faster, as per Equation 4.

$$time\ on\ recovery\ curve = -22ln\left[1 - \frac{0.67\left[29 - 10\left[\frac{RTE(i)-1}{49}\right]\right] - A(t,E)}{0.67\left[29 - 10\left[\frac{RTE(i)-1}{49}\right]\right]\left[\frac{RTE(i)-1}{49}\right]}\right]$$

Equation 4 shows the equation used to calculate the rate of recovery (Potvin & Fuglevand, 2018) of a given motor unit, where A(t,E) represents the intrinsic adaptation current, itself dependent on the length of time the motor unit has been recruited (t) and the excitation level (E).

With high intensity tasks, there is a sharp decline in motor unit capacity when compared to low intensity tasks. There are also expected differences in the recovery from fatigue in high and low intensity tasks (Figure 13).

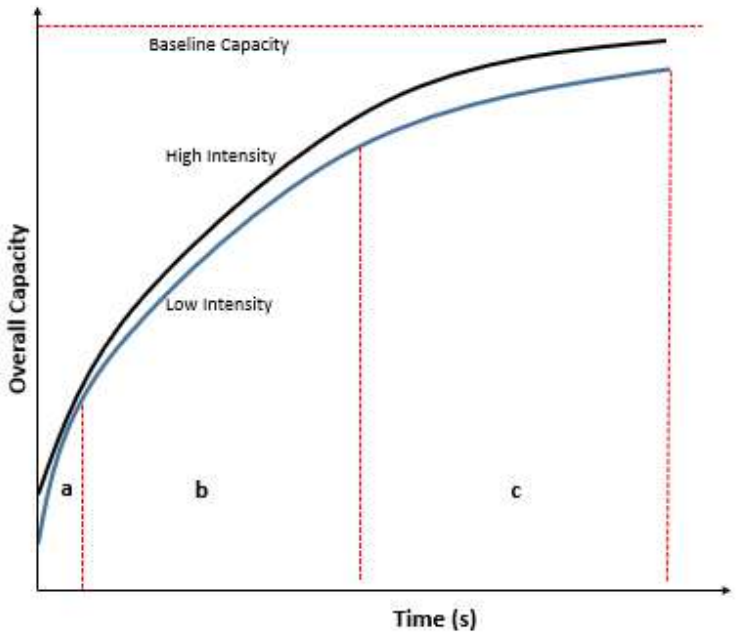

Figure 13. Difference in recovery rates from high and low intensity fatigue

The differences in the recovery from high and low intensity simulations may have been due to the extent to which the smaller motor units accumulated fatigued. For fatigue accumulation from the lower intensity, it was expected that there was an initial exponential recovery period (rapid recovery of large, very fatigued motor units) (Figure 13a), then by a linear recovery period (intermediate motor unit recovery) (Figure 13b), and finally a slower recovery of the smallest, slow twitch motor units (Figure 13c). With fatigue accumulation from the lower intensity, the initial exponential period of larger motor unit recovery (Figure 13a), and the more rapid recovery of overall capacity in the linear (Figure 13b) and plateauing (Figure 13c) regions may have been due to the shorter time period that the motor units were active compared to the lower intensity simulation.

Overall, the SPiTFiRe model informed predictions that more closely resemble the activation of muscle fibers, and their subsequent fatigue accumulation and recovery requirements. It was important to validate the assumptions made by this model, particularly the

differing recovery rates of large and small motor units, which may be preferentially activated and fatigued in response to high and low intensity activities, respectively.

3.0 Methodology

Two protocols were simulated to inform the intended experiment. First, I used the SPiTFiRe model to identify candidate force-time histories that would be likely to result in different levels of fatigue within slow-twitch motor units. Then I designed an experiment to measure recovery following exposure to the candidate force-time histories identified by the model.

3.1 Simulation of Fatigue from High and Low Intensity Tasks

This section outlines how the force-time histories were determined for low and high intensities protocols in the empirical study. The SPiTFiRe model was used to identify two force-time history patterns that would produce different amounts of fatigue in smaller, slow twitch motor units (given that large, fast twitch motor units are always fatigued when reaching the endurance limit) through trial-and-error. These two force-time histories were used in the experimental protocol.

The force-time history used to model fatigue from the low intensity task was done such that the triceps were able to meet the target contractions for a longer total endurance time, causing a relatively greater decline in the smaller motor units. These smaller motor units were expected to experience a significantly greater decline in force generating capacity relative to the high intensity protocol, the latter which was expected to result in a shorter time interval that the participant was able to maintain the target force. Muscle contractions ranging between 30-50% were seen to cause a relatively rapid decline in force generating capacity (Iridiastadi and Nussbaum, 2006; McKenzie et al., 1992; Yung et al., 2012), indicative of fatigue in larger motor units without overtly fatiguing smaller motor units. In terms of fatigue accumulation at low

intensities, Yung et al. (2012) identified that 15 %MVF sustained isometric contractions had a long term fatigue effect. Therefore, a low intensity protocol with a target force ranging between 15%MVF and 30%MVF, and a high intensity protocol with target forces above 50%MVF may generate significantly different task failure times through preferential fatigue accumulation in smaller or larger motor units, respectively. Finally, from a modelling perspective, having the overall capacity from both protocols decline to a common capacity allowed for comparisons between the two recovery profiles in the SPiTFiRe model.

From the aforementioned constraints, and through a trial-and-error approach, a 20%MVF target force (low intensity protocol) and a 70%MVF target force (high intensity protocol) were inputted into the SPiTFiRe model and were determined to be appropriate to conduct the study (Figure 14).

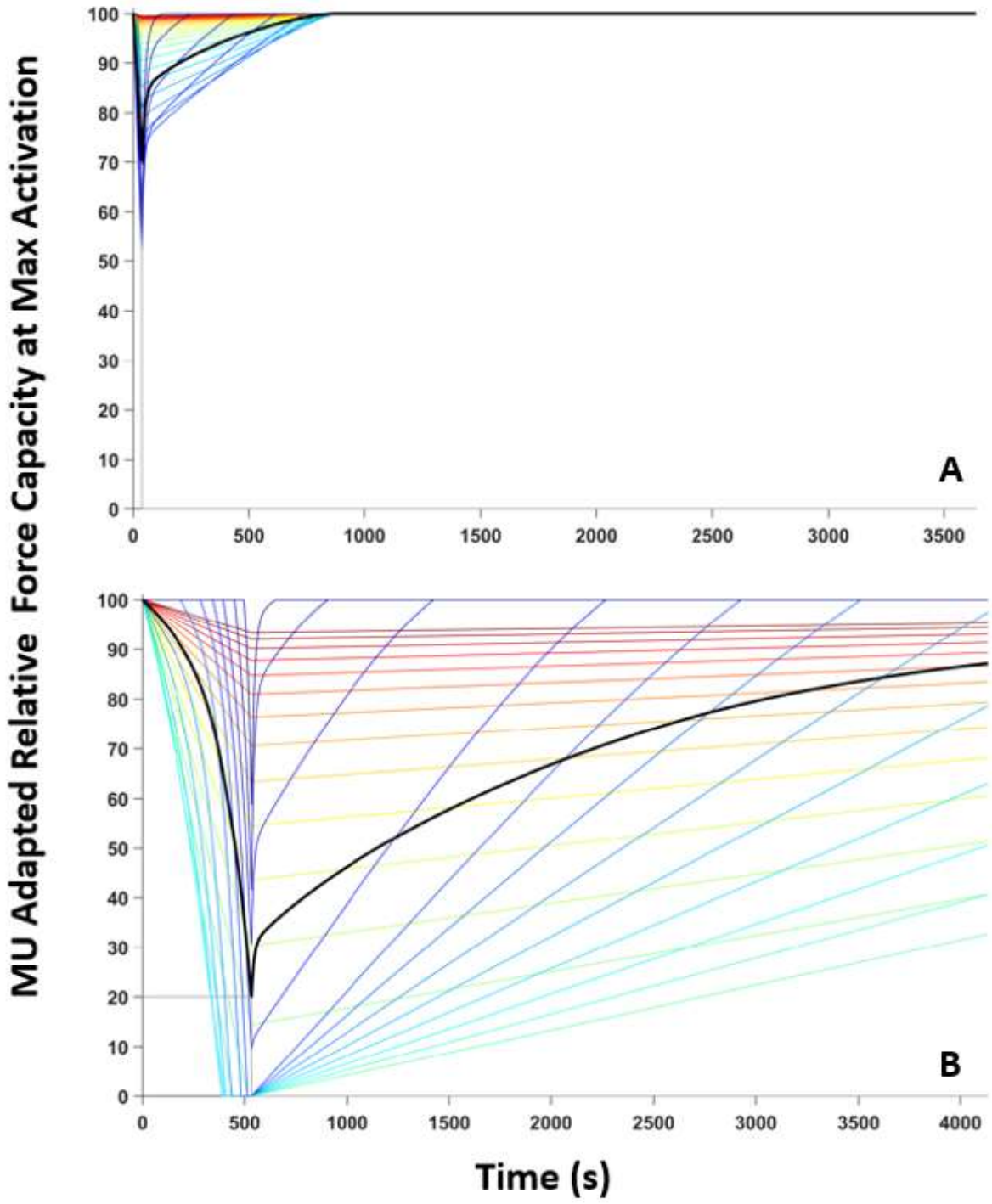

Figure 14. Simulated decline and recovery in relative force generating capacity of muscle motor units during the sustained 70 %MVF (A) and the 20% MVF (B) protocols.

Figure 14 shows the SPiTFiRe's predictions of relative contributions of the motor unit pool to generate the target forces, as well as their decline from maximum during the simulated low intensity and high intensity protocols. Upon removal of the force requirements, the model also predicted the motor unit pool's behaviour over one hour of recovery (3600 seconds). The model predicted an endurance time (time for overall capacity to fall below the target force) in the low intensity protocol of 534 seconds, while the high intensity protocol had a modelled endurance time of 37 seconds. The largest motor units (darkest blue in color), the smallest motor units (darkest red in color) and the intermediate sized motor units (lighter blue to lighter yellow in color), due to their greater overall decline, were slower to recover their overall capacity following the low intensity protocol compared to the motor unit pool in the high intensity protocol. In contrast to the low intensity protocol, the high intensity protocol saw a preferential decline in force generating capacity from the largest motor units, while the intermediate and smallest motor units experienced a comparatively lower decline. Although there was a similar period of rapid recovery following the low intensity protocol, the greater decline in smaller motor units seen in the low intensity protocol resulted in a longer recovery time.

Based on the high and low intensity protocol simulations, I simulated the overall recovery of the first eighty-three motor units in the SPiTFiRe motor unit pool following the high and low intensity protocol simulations (Figure 15). These motor units are responsible for generating a 15%MVC for one second, and were used as comparisons to the one second stimulations at 100Hz in the experimental protocol (see Section 3.2.2.3). The 100Hz stimulation was used for this comparison as it was the frequency used to elicit a 15%MVF elbow extension in the empiricial study. Comparing these modelled and empirical measures of recovery allowed us to

either explain recovery patterns in the empirical data, and/ or identify opportunities for model improvements in the SPiTFiRe.

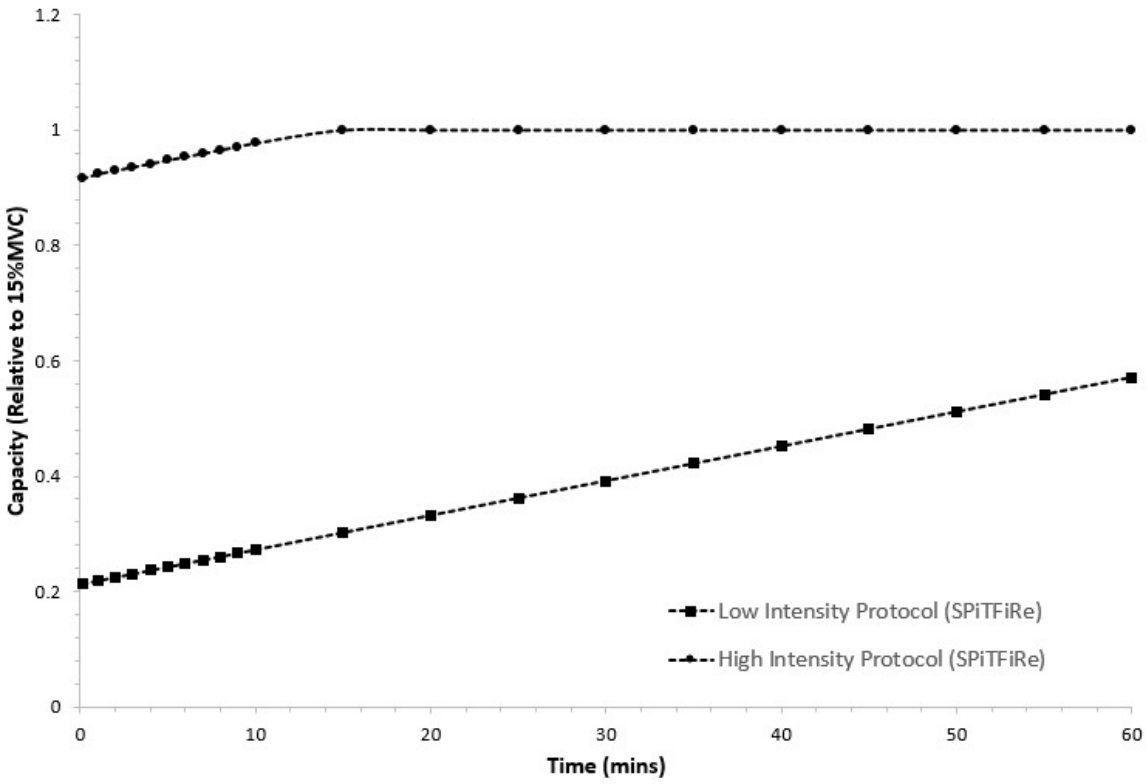

Figure 15: Recovery of motor units responsible for generating 15%MVC in the SPiTFiRe model

Prior to conducting the study, I expected that the recovery from the experimental protocols would have closely resembled the modelled outputs in Figure 15 i.e., that the average NFR following the high intensity protocol would have been higher compared to the low intensity protocol.

3.2 Experimental Methods

3.2.1 Experimental Design

A three-factor repeated measures experimental design was used to test the effects of force time history (high (70 %MVF) and low (20 %MVF) intensity), frequency (high (100 Hz) and low (20 Hz)) of stimulation, and post endurance time intervals (task failure, every minute from 1-10 minutes, and every five minutes from 15-60 minutes) on the Normalized Force Response (NFR). To conduct a three-factor, repeated measures analysis of variance (ANOVA), an a priori power analysis using the G*Power software was used to determine the sample size necessary to obtain a statistical power of 0.8 across time, intensity, and frequency, to detect a large effect difference of 0.4 at an alpha level of 0.05. A sample size of twenty-eight participants was determined to ensure that there was at least an 80% chance of correctly rejecting any non-significant differences in force response between frequency and intensity (two groups, four measurements). This sample size also ensured that any non-significant differences in the NFR between time and either intensity or frequency (two groups, forty-two measurements) are rejected as appropriate.

To wash out potential order effects, participants were block randomized such that fourteen participants performed either the high intensity or low intensity protocol on the first day, then performed the remaining protocol one week after to provide sufficient time to full recovery between fatiguing events. The study was reviewed and approved by the University of Waterloo Office of Research Ethics Committee (ORE #44194)

3.2.2 Participants

A convenience sample of twenty-eight right handed participants were recruited from a population of right-handed male (n = 14) and female (n = 14) University of Waterloo students without prior history of distal upper limb injury within the past year. Each participant performed fatiguing low and high intensity protocols on two separate days. Following this, recovery was measured through electrical stimulation at high and low frequencies (Yung et al., 2012). Table 1 summarizes the overall demographic information.

Table 1: Summary of participant demographics.

Characteristic	**Mean ± SD (Range)**
Age (years)	25.0 ± 4.0 (21.0 – 37.0)
Height (cm)	171.0 ± 9.0 (158.0 – 188.5)
Weight (kg)	72 ± 17 (48 - 116)

Prior to any personal data collection, each participant was briefed through an information letter, such that informed consent/ decision to withdraw was provided. If consent was given, and in order to ensure that all participants did not have any recent history of upper limb injury or chronic pain within the past year and are able to perform an intermittent triceps contraction protocol as a part of both low intensity and high intensity protocol, a Get Active Questionnaire

(Appendix A) and a Nordic Musculoskeletal Questionnaire (Appendix B) were completed, respectively.

3.2.2 Instrumentation

3.2.2.1 Force Transducer

A Bertec six-component load cell (PY6) was used to track the external force produced by the participant in the vertical force axis (F_z) (Bertec Corporation, 2012) (Figure 15).

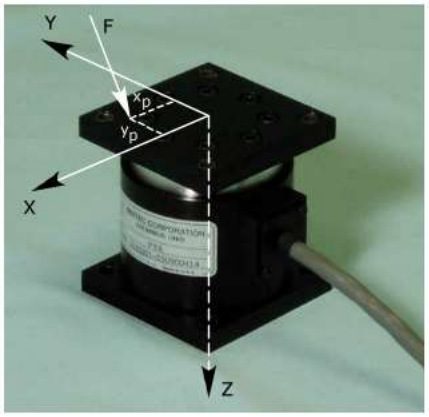

Figure 16. Bertec PY6 force transducer with attachment plates, showing the force axes (X,Y,Z) and a potential point of application of the force (F) (Bertec Corporation, 2012)

Participants were seated on an adjustable, backless seat, with their right arm on an adjustable arm rest, and their elbow oriented at 90° while holding a custom handle attachment connected to the force transducer (Figure 16).

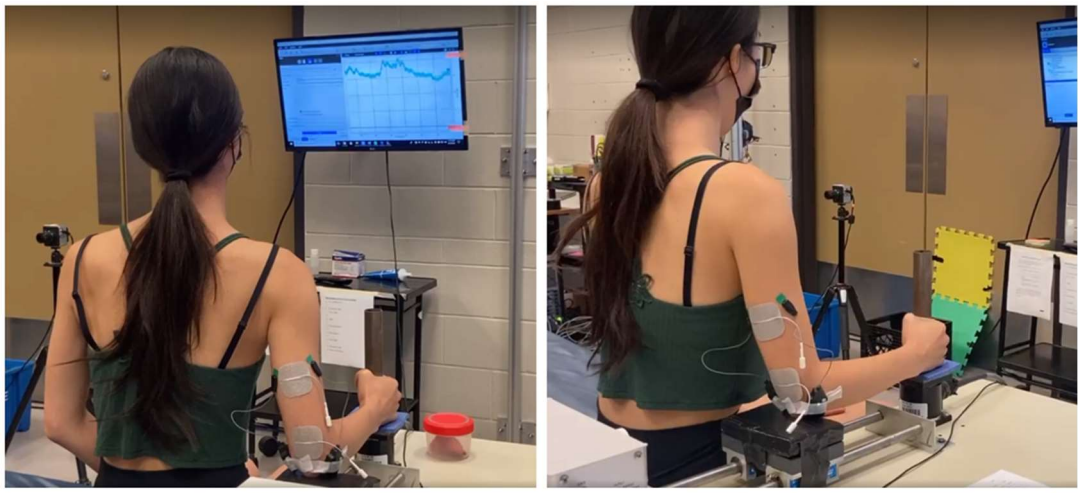

Figure 17. Participant setup for triceps contraction protocol.

3.2.2.2 Electromyography

Surface EMG was sampled at 2000Hz unilaterally from the long and lateral heads of the triceps brachii, and the biceps brachii using wireless Delsys Trigno mini sensors (Figure 18). Each electrode is bar-shaped, where specific details are outlined in Table 2.

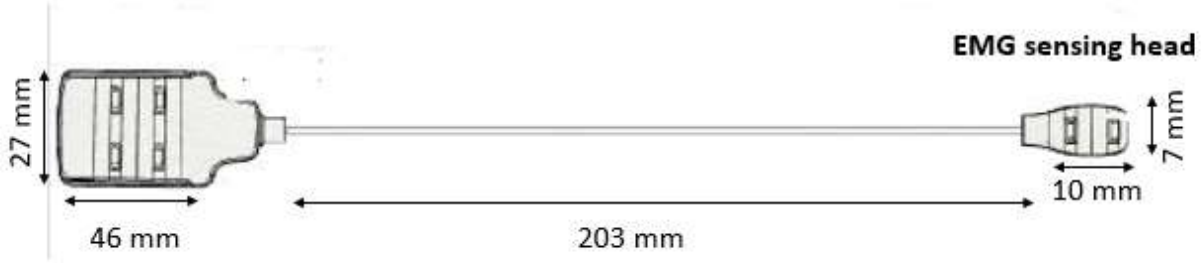

Figure 18. EMG Trigno mini sensor

Table 2. Delsys Trigno mini specifications

Input Range	+/- 11mV
Bandwidth	20-450 Hz
Maximum Sampling Rate	1926 samples/sec
Contact Material	Silver (99.99%)

Following SENIAM guidelines (Hermens et al., 1999) and Criswell (2010), each electrode was placed on the muscle bellies of interest, estimated to be in parallel with each muscle's fiber direction (Table 3). It was ensured that the skin surfaces was shaved and cleaned with 70% isopropyl alcohol, to minimise surface impedance prior to electrode placement.

Table 3. Electrode location and orientation based on the muscle of interest

Muscle	**Electrode Location**	**Electrode Orientation**
Triceps Brachii (Long head)	At 50% on the line between the posterior crista of the acromion and the olecranon; two finger widths **medial** to the line	In the direction of the line between the posterior crista of the acromion and the olecranon
Triceps Brachii (Lateral Head)	At 50% on the line between the posterior crista of the acromion and the olecranon; two finger widths **lateral** to the line	

Biceps Brachii (Long and Short Heads)	1/3 of the distance on the line between the medial acromion and the cubital fossa, from the cubital fossa	In the direction of the line between the acromion and the cubital fossa

3.2.2.3 Muscle Stimulation

A Grass S48 Muscle Electrical Stimulator with an SIU5 isolation unit (Grass Instruments, Quincy, MA) (Figure 19) was used to stimulate the triceps at 100 Hz and 20 Hz at baseline, following the performance of the MVCs, and at pre-determined time points following task failure.

Figure 19: Grass S48 Muscle Electrical Stimulator

As per the protocol outlined by Yung et al. (2012), the stimulator was connected to the proximal and distal portions of the posterior arm (Figure 18). Reusable Axelgaard PALS® 5cm x 5cm square electrodes (Figure 20) (Axelgaard Manufacturing Co, Fallbrook, CA) were connected to the muscle stimulator using SAF-P adapters.

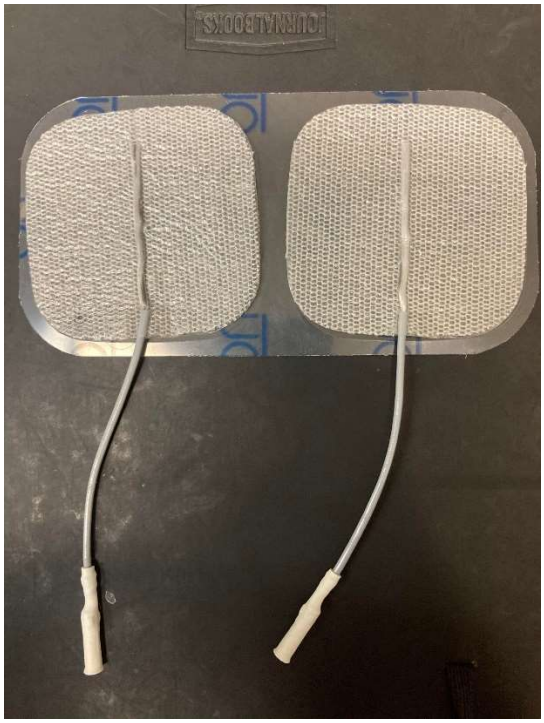

Figure 20: Axelgaard PALS® electrodes

On the participant, the proximal electrode was placed 1cm above the triceps tendon, which overlaps with both the long and lateral heads of the triceps. The distal electrode was placed 1cm above the acromion process, in line with the proximal electrode (Figure 18). This was done to obtain the pickup volume that activates the largest proportion of muscle fibers.

The muscle force outputs at each time point were collected sequentially, with the 100 Hz stimulation occurring first, followed by the 20 Hz stimulation. The settings on the stimulator and isolation unit are summarized in Table 4:

Table 4: Settings for Muscle Stimulation Unit and Isolation Unit

Machine	Setting Name	Set to
Stimulation Unit (S48)	Train Rate (Trains Per Second)	1 t/s
	Train Duration (Seconds)	1s
	Stim Rate (Hz or Pulses Per Second)	100 Hz (high frequency) 20 Hz (low frequency)
	Delay	0.01 ms
	Duration	0.05 ms
	Pulses	Single
	Voltage (V)	Adjusted for 15 %MVF at 100 Hz
Isolation Unit (SIU5)	Multiplier	X1
	Coupling	Direct
	Polarity	Normal

3.1.3 Protocol

The protocol was completed on two days, approximately one week apart (Figure 22). Each day incorporated the following protocol elements, in order: onboarding, setup of equipment to collect participant data, collecting baseline measures (MVF, MVC, NFR), performance of the fatigue protocol (either high or low intensity on a given day), and measures of recovery following fatigue (NFR) at high and low frequencies (Figure 21).

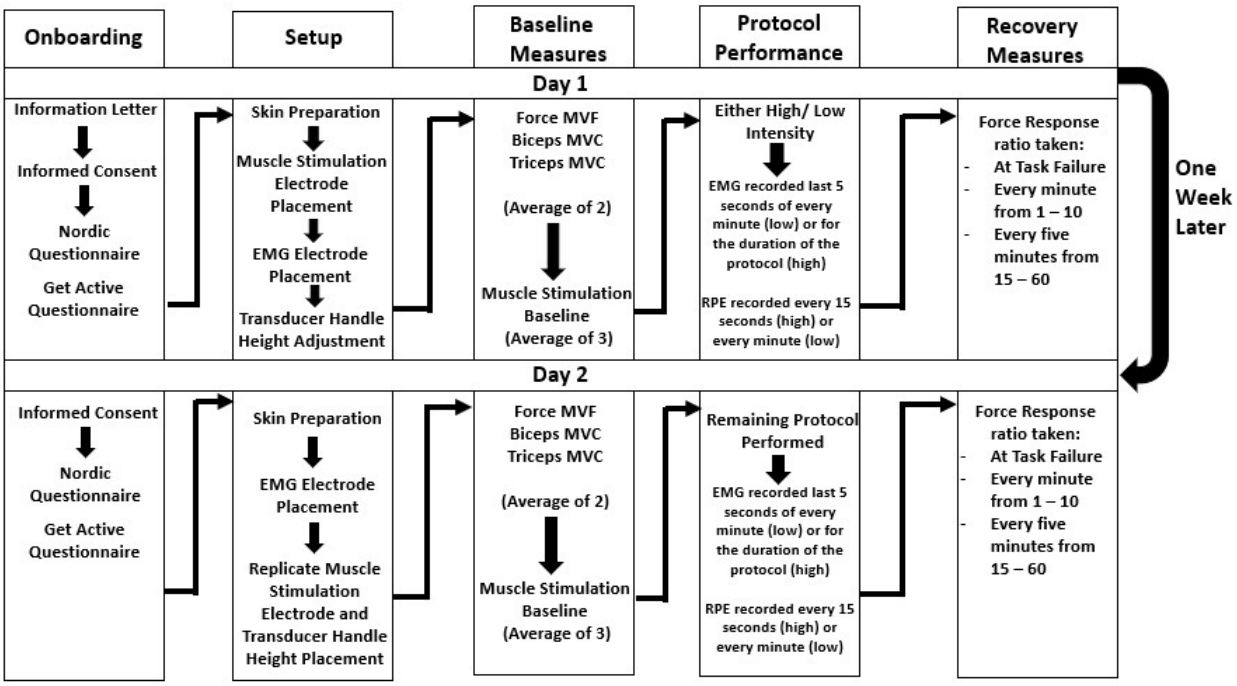

Figure 21. Flowchart of protocol elements

Before collecting baseline measures, each participant was seated, and the setup was adjusted such that their right elbow angle was at 90° when holding the handle connected to the force transducer, their elbow was supported by an adjustable arm rest, they were seated high enough that their shoulders were relaxed, and their feet were firmly supported on the stool (Figure 17). After the setup was confirmed, the arm rest length was recorded and reused for both collection days. The participant was then prepped for EMG collection, and muscle stimulation. Afterwards, while holding the handle, the participant's elbow extension MVF was recorded from the force transducer twice, with five minutes between each exertion. The average between these two efforts was recorded, and used to calculate the target forces. Following the MVF recordings, the participant's MVCs from the biceps and triceps EMG outputs were then recorded. The biceps and triceps MVCs were recorded through isometric elbow flexion and extension, respectively, with the elbow angle at 90° while being manually resisted by one of the researchers. Before the

MVF and MVCs were recorded, the participant was instructed to slowly ramp up to their maximum contraction, and were audibly encouraged during the processes to ensure maximum efforts.

At the beginning of each collection day, prior to starting each fatigue protocol, baseline muscle responses to high (100 Hz) and low (20 Hz) frequency electrical stimulations were recorded (Figure 22). These stimulations were delivered to the triceps brachii at an intensity that generated a 15% MVF at 100Hz (high frequency stimulus) while the participant held the handle connected to the force transducer. The baseline was measured three times, once per minute at the beginning of every minute, for three minutes.

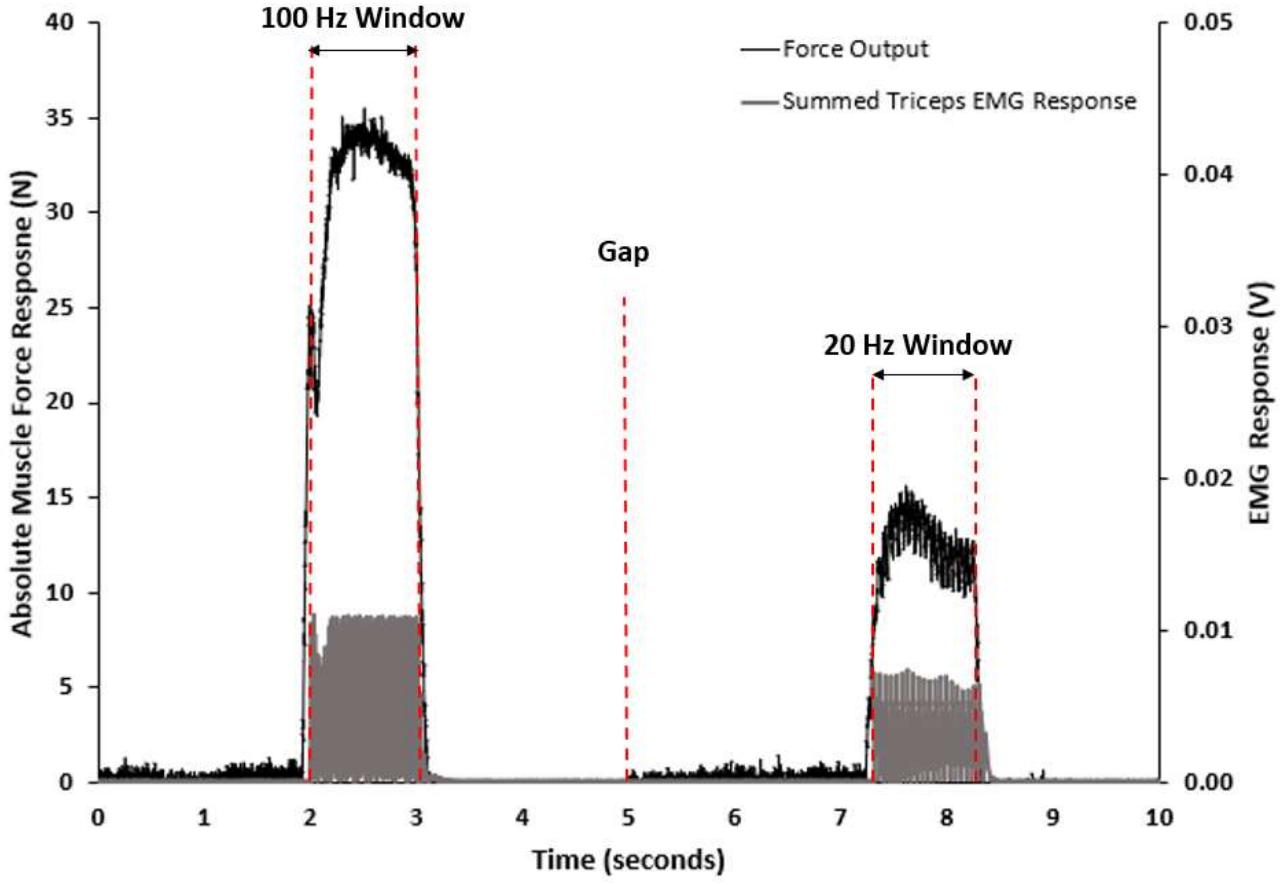

Figure 22. Raw force response from 100 Hz (left) and 20 Hz(right) triceps stimulations

Participants were given visual feedback of their voluntary force transducer output through a screen placed in front of them. EMG activity and force output from the transducer were recorded during the last five seconds of each minute of the low intensity protocol, and for the entire duration of the high intensity protocol. These data provided a secondary measure to track the activation levels of the triceps and biceps throughout both protocols. As each participant performed a fatiguing protocol, their RPE was requested every fifteen seconds (high intensity protocol) or in the final five seconds of every minute (low intensity protocol) using a Borg 6-20 scale. The protocol was terminated if a participant was either unable to sustain the target force, or provides an RPE of 20 when asked. This was considered task failure. At task failure, the endurance limit (in seconds) was recorded.

The triceps were stimulated immediately following task failure, and at the beginning of every minute from 1-10 minutes, and at the beginning of every five minutes from 15-60 minutes. EMG and force were measured during each stimulation. It was ensured that the sampling rate from the force transducer (1000 Hz) was a multiple of the sampling rate of the EMG signal (2000 Hz), such that the data could be analyzed synchronously in time. These measures were used to determine the force responses at high (100 Hz) and low (20 Hz) frequency stimulations.

3.3 Data Conditioning

Normalized Force Response through Muscle Stimulation

The raw force outputs from 100 Hz and 20 Hz stimulations were low pass filtered at 15 Hz using a second order Butterworth filter. The average muscle force response was recorded from the window in time where there was a plateau in force output during the 100Hz and 20Hz stimulations. Since the stimulating electrode was located above the EMG sensors on the long and lateral heads, the initiation of muscle contraction and subsequent force output preceded the detection of electrical stimulation (Figure 23). As a result, the initiation of these EMG signals roughly coincided with the point where the force output began to plateau (or "turning point"). Therefore, this point was used as the start of the window. To simplify this detection, the EMG response was summed before the initial start point was determined. The window was "closed" at the point where the force output fell past the force at the start of the window.

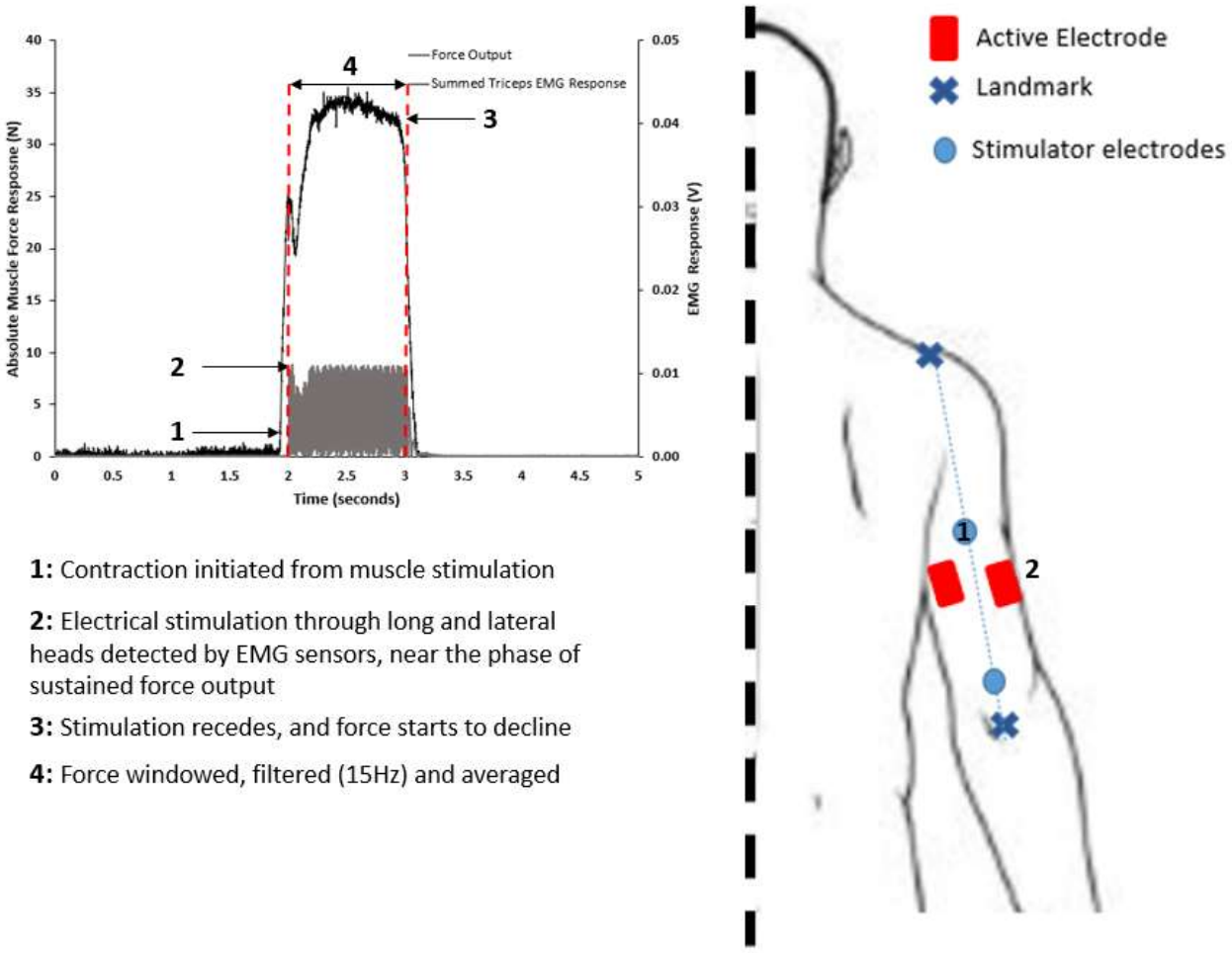

Figure 23: An outline of the windowing of force using EMG response from the long and lateral heads of the triceps

The mean force during each window was calculated as a measure of the force response at each particular frequency and time point. This mean force was then normalized to the averaged, windowed baseline force response. Statistically, these normalized force responses (NFRs) were compared across intensity, frequency, and time.

Electromyography

The EMG data were bandpass filtered between 20-450 Hz by the collecting hardware to remove any potential noise present outside of this range. The imported EMG data were processed using Python. EMG data were detrended to remove any DC bias, full wave rectified, and low pass filtered using a second order Butterworth filter at 6 Hz to generate a linear envelope (Fischer et al., 2009). The EMG recorded during the plateau phases were averaged and normalized relative to the particular muscle's average linear enveloped maximum EMG amplitude collected during the MVC trials on that day. This allowed for the calculation of the average percent activation of the muscle of interest at the time period where EMG was collected.

Equation 5 represents the calculation of a participant's average percent activation at a given time window based on the average EMG amplitude during that window (i), and the average maximum EMG amplitude obtained from the MVC trial.

$$Average\ Percent\ Activation = \frac{Average\ EMG(i)}{Average\ EMGmax} * 100\%$$

Normalization allowed for the EMG outputs to be comparable across individuals. The average percent activation from low and high intensity protocols were plotted to track the changes in amplitude across subsequent windows of time.

Since EMG data were collected across the entire high intensity protocol, it was possible to window each participant's EMG and target force data at 1%, 5%, 10%, then at intervals of 10% of their endurance time, and average the outputs across all participants. However, since EMG data were only collected for five seconds at the end of every minute for the low intensity

protocol, EMG was averaged at the recording taken at the endurance limit, as well as the recordings taken at increments of 12.5% of the endurance limit.

3.4. Statistical Analyses

A three-factor repeated measures ANOVA was performed in RStudio (RStudio Team, 2020). The RMANOVA assessed the effects of force time history (high or low intensity), frequency of stimulation (100 Hz or 20 Hz), and post endurance time interval (twenty-one levels) on the normalized muscle force responses. Bonferroni-corrected pairwise comparisons were performed to decompose main and interaction effects.

Given that a sample of twenty-eight participants was collected across two days (a total of fifty-six collections), it was likely that a Shapiro-Wilk test for normality would have generated a false-positive i.e., falsely indicating that the force response may not follow a normal distribution (Ghasemi and Zahediasl, 2012). However with a large sample size, it was deemed appropriate to perform a parametric three-way RMANOVA, and visualize the normality of the distribution of data across intensity, frequency, and time, using Quantile-Quantile (Q-Q) plots (Pallant, 2011; Uttley, 2019).

Additionally, a two-factor repeated measures ANOVA was performed to verify whether there were any significant differences in the average MVFs pre- and post- protocol completion, between high and low intensities. Bonferroni corrected pairwise comparisons were then performed to determine which sub-groups were different/ not different across groupings of protocol (high versus low) and time (pre versus post).

4.0 Results

4.1 Summary of Participant Performance

The average endurance time for the low intensity protocol was 838.3s, which exceeded the average endurance time following the high intensity protocol (62.5s) (Table 5). Additionally, there was large standard deviations in the low intensity protocol endurance time compared to the high intensity protocol, noted by differences in coefficients of variation.

Table 5: Descriptive statistics for maximum voluntary force, stimulation voltage, and endurance time stratified by protocol.

	High Intensity Protocol (n = 28)	**Low Intensity Protocol (n = 28)**
MVF (Pre-Protocol) (N)	150.2±46.9 (70.2-242.0)	151.3±47.5 (77.1-248.8)
MVF (Post-Recovery) (N)	144.7±44.4 (75.2-149.6)	149.5±27.3 (67.3-252.0)
Average Stimulation Voltage (V)	117.3±20.8 (70.0-150.0)	114.8±19.0 (75.0-150.0)
Endurance Time (s)	62.5±24.5 (32.0-143.0)	838.3±512.4 (360.0-2700.0)
Coefficient of Variation	0.39	0.61

The performed ANOVA resulted in a significant main effect of time ($F(1,27) = 6.210$, $p = 0.019$, $\eta_p^2 = 0.187$). There was no significant main effect of the performed protocol ($F(1,27) = 0.617$, $p = 0.439$, $\eta_p^2 = 0.022$) nor was there a significant interaction effect ($F(1,27) = 1.742$,

$p = 0.198$, $\eta_p^2 = 0.061$). Pairwise comparisons identified no significant difference in average MVF prior to the high versus low intensity protocol ($t = 0.287$, $df = 27$, $p>0.05$). Additionally, with regards to the low intensity protocol, there was no significant difference in average MVF prior to the fatigue protocol and following one hour of recovery ($t = 1.213$, $df = 27$, $p>0.05$). However, with regards to the high intensity protocol, the average post-protocol MVF following the recovery period was significantly lower than the average pre-protocol MVF ($t = 2.280$, $df = 27$, $p = 0.031$). These comparisons were visualized in Figure 24.

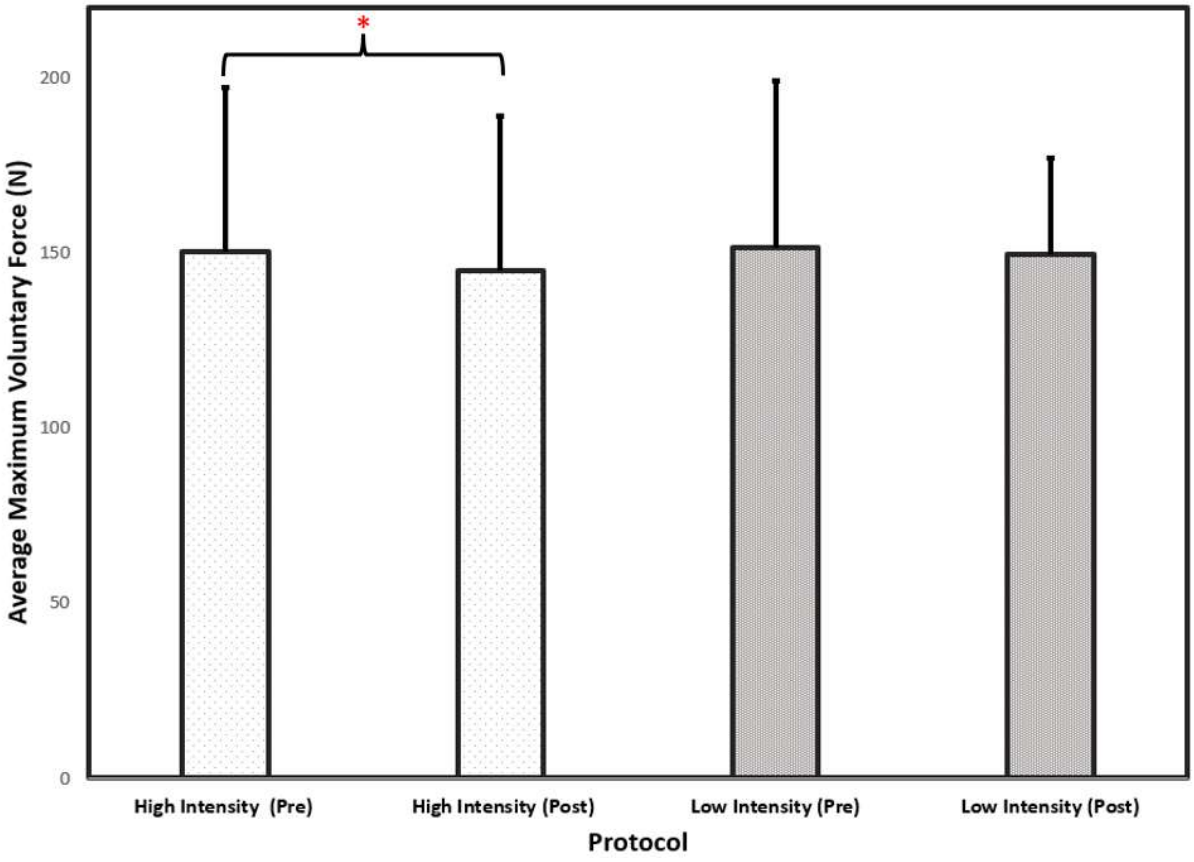

Figure 24: Average MVF outputs stratified by intensity (high versus low) and time (pre versus post)

4.2 Triceps Force Response to Electrical Stimulation Following Task Failure

Intensity and stimulation frequency each interacted with time to effect observed NFR, but no intensity by stimulation frequency by time interactions were observed (Table 6). Specifically, the RMANOVA detected a significant interaction between intensity and time ($F(6.0,162.8) = 12.94$, $p < 0.001$, $\eta_p^2 = 0.32$), and between frequency and time ($F(8.64,233.29) = 6.92$, $p < 0.001$, $\eta_p^2 = 0.20$). An illustration of the NFR across all combinations of intensity and frequency can be found in Appendix C, Figure 33.

Table 6: Results from the Three-Way Repeated Measures Analysis of Variance

Effect	Degrees of Freedom (n,d)	F statistic	Partial Eta Squared	Adjusted p value (Bonferroni)
Intensity	1.00,27.00	0.42	0.02	1.00
Frequency	1.00,27.00	72.91	0.73	$p < 0.001$
Time	6.50,175.53	30.10	0.53	$p < 0.001$
Intensity x Frequency	1.00,27.00	0.89	0.03	1.00
Intensity x Time	6.20,167.37	12.94	0.32	$p < 0.001$
Frequency x Time	8.64,233.29	6.92	0.20	$p < 0.001$
Intensity x Frequency x Time	8.47,228.63	1.07	0.04	1.00

Post-hoc pair wise comparisons to decompose the intensity by time interaction revealed that the NFR (collapsed across stimulation frequency) was initially higher (0-4 minutes) following the high intensity protocol relative to the low intensity protocol, but then declined and was lower than the NFR following the low intensity protocol (from 10-30 minutes) before returning to a similar NFR as the recovery time approached 60 minutes (Figure 25), with the NFR being significantly different at minutes 35 and 60. A table with p-values for pairwise comparisons is included in Appendix D, Table 8. In contrast, post-hoc pairwise comparisons to decompose the frequency by time interaction revealed that the NFR (collapsed across task

intensity) remained higher from minutes 0-60 following high frequency stimulation compared to low frequency stimulation (Figure 26). A table with p-values for pairwise comparisons is included in Appendix D, Table 10. Additionally, Appendix E presents the NFR data that were used to perform the statistical analyses in this section.

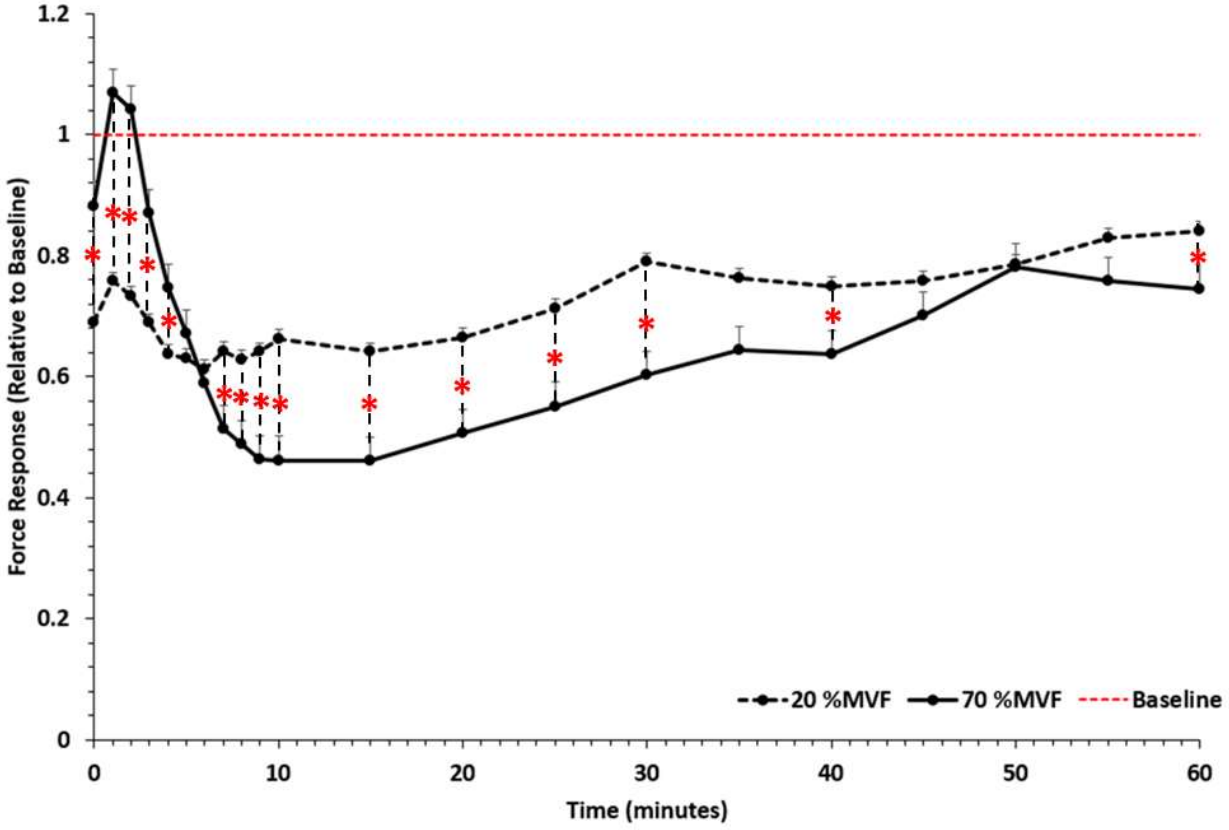

Figure 25: NFRs during recovery following completion of the high and low intensity fatigue protocols (collapsed across stimulation frequency). The vertical dashed line represents the baseline force response for reference. '' = Significantly different pairwise comparison between intensities specific to each time point.*

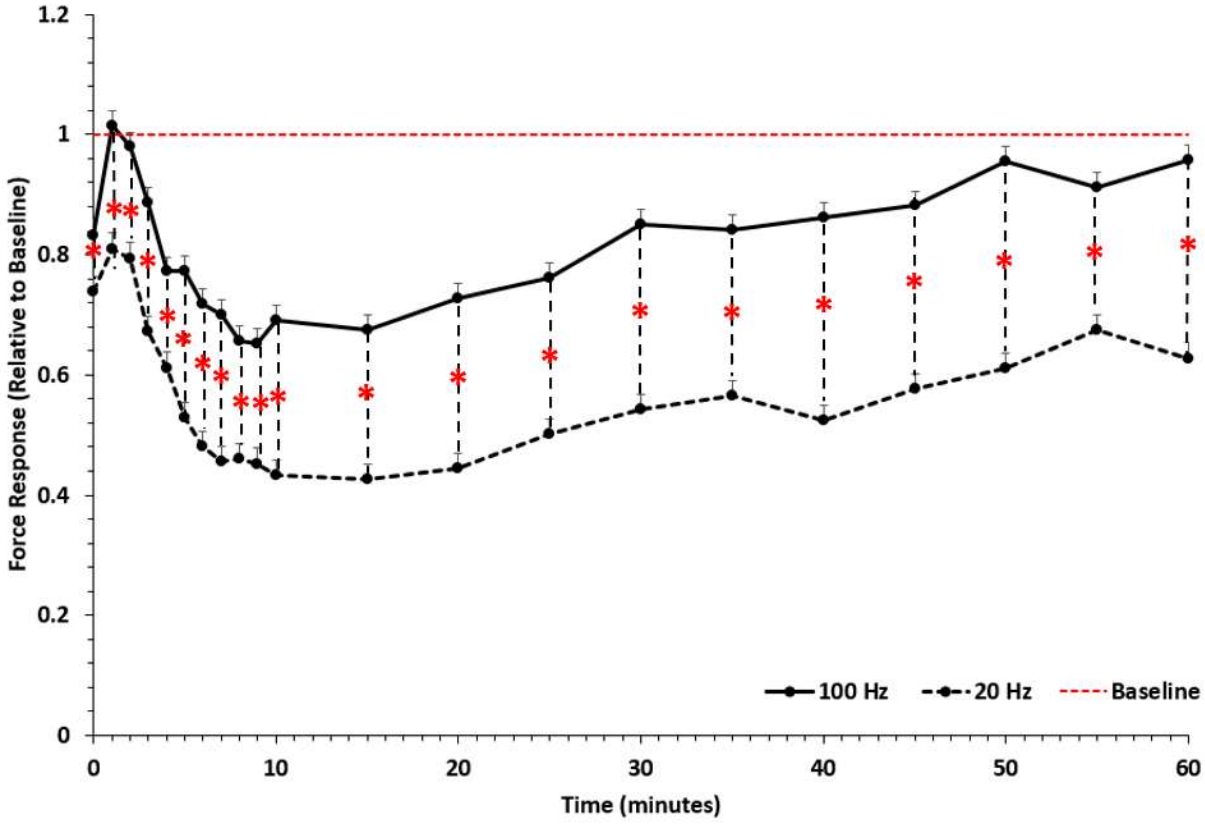

Figure 26: NFRs measured at high and low frequency stimulations during recovery (collapsed across intensity). The vertical dashed line represents the baseline force response for reference. '' = Significantly different pairwise comparison*

4.3 Muscle Activation Characteristics

Electromyography data were recorded as a secondary measure. From the Electromyography data, the average percent activation of the long head of the triceps, the lateral head of the triceps, and the biceps brachii were determined across both protocols. For the high intensity protocol (Figure 27), the percent activation of the long and lateral heads of the triceps trended upwards as participants continued to sustain the 70%MVF target force. As the protocol approached 90% of the average overall endurance time, participants were unable to sustain the target force, which declined in tandem with a declining trend in both long and lateral head percent activation levels.

Additionally, the activation level of the biceps brachii remained relatively constant throughout the duration of the protocol.

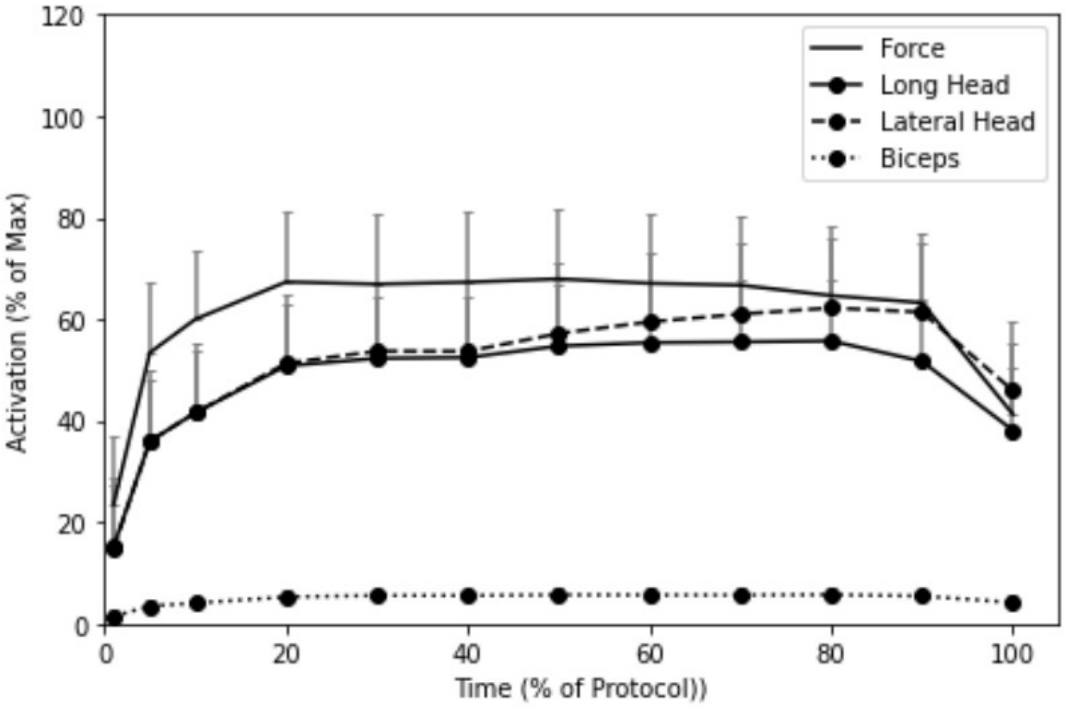

Figure 27: Average percent activation of triceps brachii and biceps brachii during high intensity protocol across all participants

For the low intensity protocol (Figure 28), the percent activation of the long and lateral heads of the triceps also trended upwards as participants continued to sustain the 20%MVF target force, though this upward trend was more linear compared to the initial plateau in muscle activation levels in during the high intensity protocol. The percent activation of the biceps brachii also remained relatively constant, similar to what was seen during the high intensity protocol. However, unlike the high intensity protocol, there was not a noticeable decline in the participant's ability to maintain the target force as the participant approached task failure.

Appendix F gives a more detailed breakdown of the average percent activations used to generate Figure 27 and Figure 28.

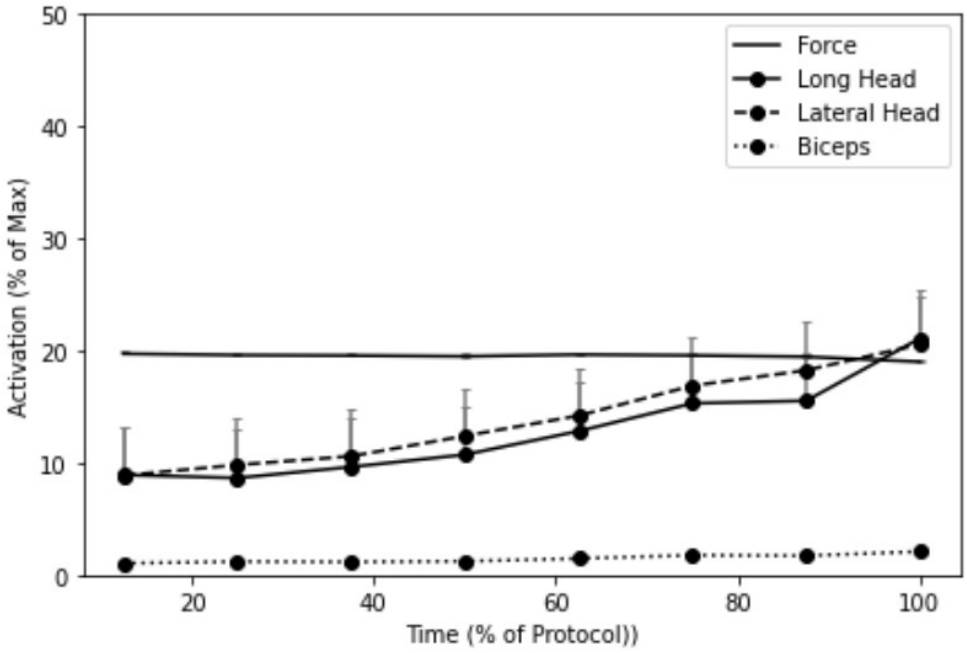

Figure 28: Average percent activation of triceps brachii and biceps brachii during low intensity protocol across all participants

5.0 Discussion

The purpose of this thesis was to determine whether the normalized force response (NFR) at post endurance time intervals differed between fatigue caused by the performance of a low intensity task versus a high intensity task. Data supported the hypothesis that the NFR at each time point would be greater following the 100 Hz stimulation compared to the 20 Hz stimulation, indicating that a higher frequency of motor unit stimulation was required to generate force relative to pre-fatigue baseline. However, data did not support the hypothesis that the NFR at each time point would be greater following the 70%MVF fatigue protocol compared to the 20%MVF fatigue protocol. While there was a clear pattern in the differences in the NFR when comparing 100Hz and 20Hz frequencies over time, the differences in recovery following fatigue at high and low intensities were more nuanced.

There was a rise in the NFR following the first minute of recovery for all combinations of intensity and frequency. While this sudden rise in force may be physiologically driven (Miyamoto et al., 2012; Smith et al., 2013), exercise-induced temperature and sweat increases have been shown to increase skin conductance to electrical stimulation (Bîrlea et al., 2014), which would have dissipated as participants began to cool down. The increase in sweat in particular may also be greater following higher intensity efforts (Machado et al., 2018), which may explain the greater peak in NFR following task failure after the 70%MVF protocol. The sharp rise in force following task failure was followed by a force depression of a greater magnitude during recovery from the high intensity protocol versus the low intensity protocol. This force depression following potentiation has been attributed to either a loss in muscle excitation due to sarcolemmal Na^+/K^+ pump impairments (Allen et al., 2008; Fowles et al., 2002;

McFadden and McComas, 1996) or due to impairments in the sarcoplasmic reticulum Ca^{2+} pump (Tupling et al., 2000). Through either pathway, and though alternative mechanisms may exist (Smith et al., 2013), there is a decreased availability of free Ca^{2+} to drive cross bridge formation and force generation (Tupling et al., 2000). From the observed results, the depression in the NFR was greater following the 70%MVF protocol. This may infer that physiological impairments inhibiting force generation are greater following task failure at higher intensities compared to lower intensities, though the duration of muscle activity may be much shorter.

NFRs generated from 20Hz stimulations were below baseline measures following both fatigue protocols. This deviated from the expectation that the 20Hz NFR following the 70%MVF protocol would not have been significantly lower than baseline following task failure, as the smaller recruited motor units would have been more resistant to fatigue accumulation at higher intensities and shorter durations (Dennerlein et al., 2003; Potvin and Fuglevand, 2017a). However, the 20Hz NFRs following both fatigue protocols appeared to remain below baseline at the end of the sixty minute recovery window, whereas the 100Hz NFRs appeared to recover force responses equivalent to what was measured at baseline. This may suggest that there is an impairment in smaller motor unit force generation following task failure at high intensities as well as low intensities. The recruited motor units required a higher stimulation frequency (100Hz) to generate forces that were closer to baseline levels at the same input volage, whereas the low frequency response (20Hz) was lower at each time point. This indicated that long-term low frequency mechanisms characteristic of smaller motor unit fatigue accumulation may have contributed to the reduced NFR relative to baseline (Fuglevand et al., 1999; Jones, 1996) across time, and statistically independent of the intensity of isometric effort. Additionally, recovery of the 100Hz NFR at both intensities at the end of the recovery period allowed for the recovery of

the average participant's maximum force generating capacity compared to pre task failure levels. These findings may infer that long term effects of smaller motor unit fatigue accumulation may still be present, though MVF measures return to pre-fatigue baselines.

The findings from this study provide evidence that potentiation and post-potentiation depression of the normalized force response plays an important role in recovery. This is particularly true when fatigue develops under higher intensities of effort, and has important implications for how we model fatigue recovery. The mechanism driving the modelled increase in force capacity (Potvin and Fuglevand, 2018, 2017), however, is different from the proposed mechanisms that elicited the potentiation responses in the experimental protocol (Figure 30). Additionally, the modelled overall rise in force appears to be lower following the lower intensity protocol, due to the concurrent decline in smaller motor unit capacity. However, the model presents a curvilinear recovery profile that may overestimate the actual recovery of muscle during the period where force begins to decline following potentiation. Additionally, smaller motor units have been modelled to be more resistant to fatigue at higher intensities. In contrast, force depression was observed during recovery at both intensities and also at lower frequencies, indicative of an impairment in smaller motor unit force-generating capacity. Therefore, incorporating factors of force potentiation and force depression into the SPiTFiRe model may improve the accuracy of recovery predictions from sustained efforts.

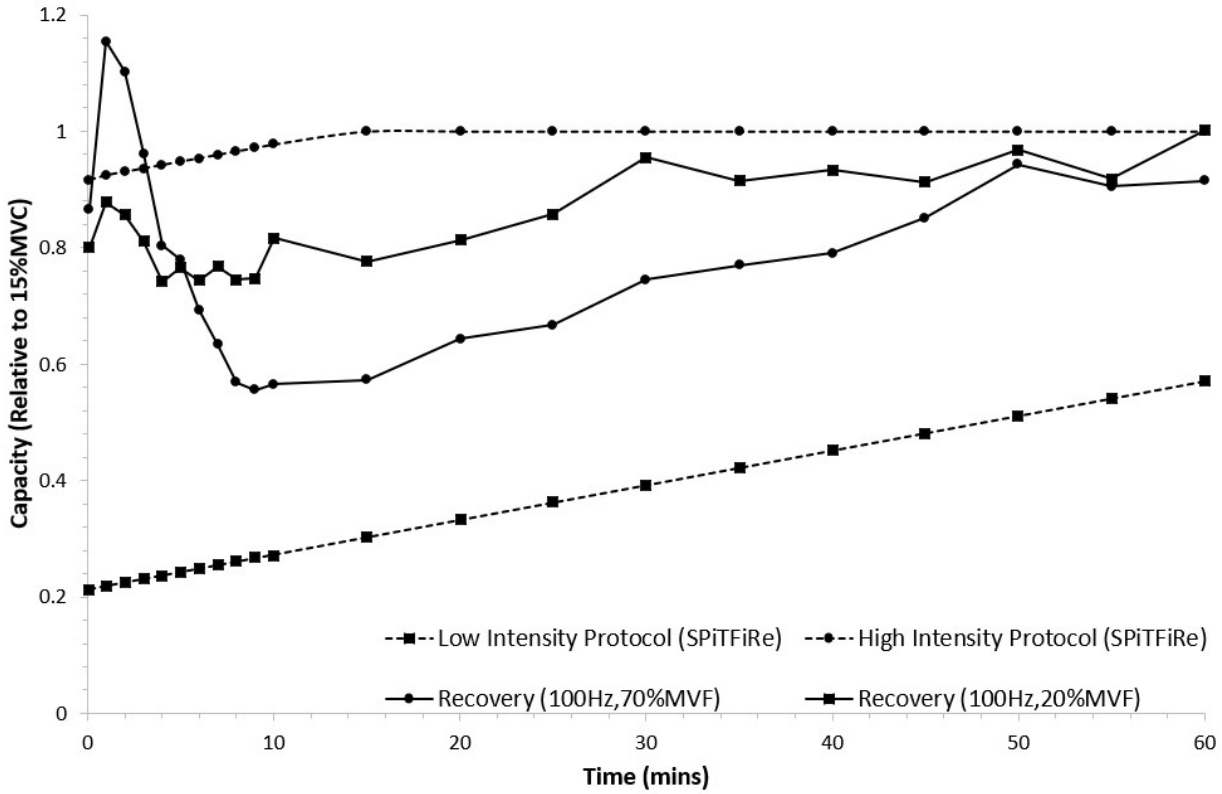

Figure 29: Comparisons between the overall muscle stimulation-measured recovery and SPiTFiRe-simulated recovery from fatigue accumulation following 20%MVF and 70%MVF protocols, normalized to baseline.

Aside from the neurophysiological differences discussed above, there are several assumptions that may have driven the observed differences between experimental versus modelled recovery profiles. The SPiTFiRe model estimated the changes in maximum muscle force generating capability, while the experimental protocol tested for changes in submaximal force generating capability. While I attempted to compare experimental outputs to a specific sub-population of modelled motor units (Figure 30), comparing the supramaximal twitch force post task failure may elicit a recovery profile following the potentiation and depression phase that more closely resembled the SPiTFiRe-modelled outputs. Additionally, the proportion of larger

versus smaller motor units that were modelled by the SPiTFiRe (Fuglevand et al., 1993) are different from that seen in the heads of the triceps (Lucas-Osma and Collazos-Castro, 2009). While the lateral head of the triceps were reported to contain predominantly smaller motor units, similar to the model, the long head of the triceps was reported to contain a balance of larger and smaller motor units (Lucas-Osma and Collazos-Castro, 2009). This may be important to consider given the contribution of both long and lateral heads to force generation during both 70%MVF and 20%MVF protocols. Finally, whereas the SPiTFiRe modelled a decline in force generating capacity past the target forces, the experimental fatigue protocol was terminated if the participant was unable to maintain the target force, or was unable to tolerate the pain associated with maintaining the force. This may reduce the proportion larger motor unit recruitment and fatigue accumulation, particularly during the 20%MVF protocol where a drop-off in force near the endurance limit was not seen. Understanding how and why modeled results differ from empirical findings may help to inform continued work to develop tools that can robustly estimate fatigue and recovery needs in the workplace.

The force profiles during the high and low intensity protocols seemed to differ as participants neared their endurance limits (Figure 27 and Figure 28). Participants, on average, seemed to be able to hold the low intensity target force until task failure. In contrast, there seemed to be a deviation from the target force following the high intensity protocol as the average participant neared their endurance limit. This provides some indication that the mechanisms of task failure may have differed. As a result, the differences in recovery profiles between high and low intensity protocols may have been due to differences in the loss of overall capacity. Therefore, a better comparison between recovery from high and low intensity task failure could have been made if each participant continued the high intensity protocol until they

could no longer maintain 20%MVF, rather than from discontinuing the task volitionally. Incorporation of measures such as electroencephalography (EEG) may help us better understand the contributions of the central nervous system, particularly to explain the differences in activation behaviour in the triceps to sustain a lower versus higher intensity isometric contraction.

Several factors may have affected the accuracy of results in our study. Caffeine intake, which has been shown to mitigate the effects of force depression following fatigue accumulation (Tupling et al., 2000) was not accounted for in the inclusion/ exclusion criteria. Caffeine results in an increase in available free Ca2+ available to bind to troponin, allowing for a greater NFR than would have been possible without the effects of caffeine (Allen et al., 2008; Tupling et al., 2000). Furthermore, since the magnitude of sweat and temperature increases following exercises may vary due to heat acclimation and training history, less adapted participants may have shown a greater degree of conductivity post task failure (Bîrlea et al., 2014; Roberts et al., 1977). Furthermore, the accuracy of the participant's elbow angle could have been improved using a goniometer. Not using a goniometer could have resulted in less error versus relying on experimenter verification of elbow angle. This error in position could have also been quantified using motion capture, which may have strengthened the validity of our findings. Finally, the stimulation at t = 0 occurred several seconds after the participants reached task failure. This may have resulted in the inability to observe the initial stages of potentiation, which may have shown a lower overall NFR.

In conclusion, I was able to determine that a higher intensity (70%MVF) isometric triceps contraction underwent a depression in the measured normalized force response (NFR) following task failure that was greater than what was observed following the lower intensity (20%MVF)

task, such that the NFR remains significantly lower up to thirty minutes following task failure. I also observed that the triceps NFR due to low frequency (20Hz) stimulation was lower than the NFR from high frequency (100HZ) stimulation, indicating that overall fatigue accumulation may be driven by low frequency fatigue accumulation in smaller motor units. However, these smaller units may accumulate substantial fatigue following task failure at higher intensities as well as lower intensities, which could be incorporated into the SPiTFiRe model to improve predictions. Overall, these findings may contribute towards addressing the future directions proposed by Veerasammy et al.(2022), where an understanding of the intensity-dependent nature of muscle fatigue recovery may advance our ability to further develop tools that estimate the accumulation and mitigation of worker muscle fatigue. Incorporation of force potentiation and force depression factors into well-known, robust tools of muscle fatigue accumulation and recovery may take us one step further towards estimating MSD risk from fatigue-related metrics.

References

Adamo, D.E., Khodaee, M., Barringer, S., Johnson, P.W., Martin, B.J., 2009. Low mean level sustained and intermittent grip exertions: Influence of age on fatigue and recovery. Ergonomics 52, 1287–1297. https://doi.org/10.1080/00140130902984935

Allen, D.G., Lamb, G.D., Westerblad, H., 2008. Skeletal muscle fatigue: Cellular mechanisms. Physiol. Rev. 88, 287–332. https://doi.org/10.1152/physrev.00015.2007

Bertec Corporation, 2012. Bertec PY6 Load Cell. Colombus, Ohio, United States of America.

Bigland-Ritchie, B., 1981. EMG/force relations and fatigue of human voluntary contractions. Exerc. Sport Sci. Rev. 9, 75–117. https://doi.org/10.1249/00003677-198101000-00002

Bigland-Ritchie, B., Woods, J.J., 1984. Changes in muscle contractile properties and neural control during human muscular fatigue. Muscle Nerve 7, 691–699. https://doi.org/10.1002/mus.880070902

Bigland Ritchie, B., Jones, D.A., Hosking, G.P., Edwards, R.H.T., 1978. Central and peripheral fatigue in sustained maximum voluntary contractions of human quadriceps muscle. Clin. Sci. Mol. Med. 54, 609–614. https://doi.org/10.1042/cs0540609

Binder-Macleod, S.A., Russ, D.W., 1999. Effects of activation frequency and force on low-frequency fatigue in human skeletal muscle. J. Appl. Physiol. 86, 1337–1346. https://doi.org/10.1152/jappl.1999.86.4.1337

Bîrlea, S.I., Breen, P.P., Corley, G.J., Bîrlea, N.M., Quondamatteo, F., Ólaighin, G., 2014. Changes in the electrical properties of the electrode-skin-underlying tissue composite during a week-long programme of neuromuscular electrical stimulation. Physiol. Meas. 35, 231–252. https://doi.org/10.1088/0967-3334/35/2/231

Briggs, A.M., Cross, M.J., Hoy, D.G., Sànchez-Riera, L., Blyth, F.M., Woolf, A.D., March, L., 2016. Musculoskeletal Health Conditions Represent a Global Threat to Healthy Aging: A Report for the 2015 World Health Organization World Report on Ageing and Health. Gerontologist 56, S243–S255. https://doi.org/10.1093/geront/gnw002

Cavuoto, L., 2016. Understanding fatigue and the implications for worker safety. ASSE Prof. Dev. Conf. Expo. https://doi.org/10.1016/0026-0657(92)91817-4

Chiang, J., Stephens, A., Potvin, J., 2008. Automotive manufacturing task analysis: An integrated approach. SAE Tech. Pap. https://doi.org/10.4271/2008-01-1897

Côté, J.N., 2014. Adaptations to neck/shoulder fatigue and injuries. Adv. Exp. Med. Biol. 826, 205–228. https://doi.org/10.1007/978-1-4939-1338-1_13

Côté, J.N., Mathieu, P.A., Levin, M.F., Feldman, A.G., 2002. Movement reorganization to compensate for fatigue during sawing. Exp. Brain Res. 146, 394–398. https://doi.org/10.1007/s00221-002-1186-6

Criswell, E., 2010. Cram's introduction to surface electromyography, 2nd ed. Jones & Bartlett Publishers, Sudbury, Massacheusetts.

Dempsey, P.G., Kocher, L.M., Nasarwanji, M.F., Pollard, J.P., Whitson, A.E., 2018. Emerging ergonomics issues and opportunities in mining. Int. J. Environ. Res. Public Health 15. https://doi.org/10.3390/ijerph15112449

Dennerlein, J.T., Ciriello, V.M., Kerin, K.J., Johnson, P.W., 2003. Fatigue in the forearm resulting from low-level repetitive ulnar deviation. Am. Ind. Hyg. Assoc. J. 64, 799–805. https://doi.org/10.1080/15428110308984875

Enoka, R.M., 2019. Physiological validation of the decomposition of surface EMG signals. J. Electromyogr. Kinesiol. 46, 70–83. https://doi.org/10.1016/j.jelekin.2019.03.010

Enoka, R.M., Duchateau, J., 2016. Translating Fatigue to Human Performance. Physiol. Behav. 176, 139–148. https://doi.org/10.1249/MSS.0000000000000929.Translating

Enoka, R.M., Duchateau, J., 2008. Muscle fatigue: What, why and how it influences muscle function. J. Physiol. 586, 11–23. https://doi.org/10.1113/jphysiol.2007.139477

Fischer, S.L., Wells, R.P., Dickerson, C.R., 2009. The effect of added degrees of freedom and handle type on upper limb muscle activity during simulated hand tool use 52, 25–35. https://doi.org/10.1080/00140130802479895

Fitts, R.H., 1994. Cellular Mechanisms of Muscle Fatigue.

Fowles, J.R., Green, H.J., Tupling, R., O'Brien, S., Roy, B.D., 2002. Human neuromuscular fatigue is associated with altered Na+-K+-ATPase activity following isometric exercise. J. Appl. Physiol. 92, 1585–1593. https://doi.org/10.1152/japplphysiol.00668.2001

Frey-Law, L.A., Schaffer, M., Urban, F.K., 2021. Muscle fatigue modelling: Solving for fatigue and recovery parameter values using fewer maximum effort assessments. Int. J. Ind. Ergon. 82, 103104. https://doi.org/10.1016/j.ergon.2021.103104

Frontera, W.R., Ochala, J., 2015. Skeletal Muscle: A Brief Review of Structure and Function. Behav. Genet. 45, 183–195. https://doi.org/10.1007/s00223-014-9915-y

Fuglevand, A.J., Macefield, V.G., Bigland-Ritchie, B., 1999. Force-frequency and fatigue properties of motor units in muscles that control digits of the human hand. J. Neurophysiol. 81, 1718–1729. https://doi.org/10.1152/jn.1999.81.4.1718

Fuglevand, A.J., Winter, D.A., Patla, A.E., 1993. Models of recruitment and rate coding organization in motor-unit pools. J. Neurophysiol. 70, 2470–2488. https://doi.org/10.1152/jn.1993.70.6.2470

Gallagher, S., Schall Jr, M.C., 2017. Musculoskeletal disorders as a fatigue failure process: evidence, implications and research needs. Ergonomics 60, 255–269. https://doi.org/10.1080/00140139.2016.1208848

Gallagher, S., Schall, M.C., Sesek, R.F., Huangfu, R., 2017. Job Rotation as a Technique for the Control of MSDs : A Fatigue Failure Perspective 993–994. https://doi.org/10.1177/1541931213601730

Gates, D.H., Dingwell, J.B., 2008. The effects of neuromuscular fatigue on task performance during repetitive goal-directed movements. Exp. Brain Res. 187, 573–585.

https://doi.org/10.1007/s00221-008-1326-8

Ghasemi, A., Zahediasl, S., 2012. Normality tests for statistical analysis: A guide for non-statisticians. Int. J. Endocrinol. Metab. 10, 486–489. https://doi.org/10.5812/ijem.3505

Gregory, C.M., Bickel, C.S., 2005. Recruitment patterns in human skeletal muscle during electrical stimulation. Phys. Ther. 85, 358–364. https://doi.org/10.1093/ptj/85.4.358

Hägg, G.M., Åström, A., 1997. Load pattern and pressure pain threshold in the upper trapezius muscle and psychosocial factors in medical secretaries with and without shoulder/neck disorders. Int. Arch. Occup. Environ. Health 69, 423–432. https://doi.org/10.1007/s004200050170

Hales, J.P., Gandevia, S.C., 1988. Assessment of maximal voluntary contraction with twitch interpolation: an instrument to measure twitch responses. J. Neurosci. Methods 25, 97–102. https://doi.org/10.1016/0165-0270(88)90145-8

Hamada, T., Kimura, T., Moritani, T., 2004. Selective fatigue of fast motor units after electrically elicited muscle contractions. J. Electromyogr. Kinesiol. 14, 531–538. https://doi.org/10.1016/j.jelekin.2004.03.008

Henneman, E., 1957. Relation between size of neurons and their susceptibility to discharge. Science (80-.). 126, 1345–1347. https://doi.org/10.1126/science.126.3287.1345

Henneman, E., Sonjen, G., Carpenter, D., 1965. Functional Significance of Cell Size in Spinal Motoneurons. J. Neurophysiol. 28, 560–580. https://doi.org/10.1152/jn.1965.28.3.560

Hermens, H.J., Freriks, B., Merletti, R., Stegeman, D., Blok, J., Rau, G., Disselhorst-Klug, C., Hägg, G., 1999. European recommendations for surface electromyography. Roessingh Res. Dev. 8, 13–54.

Hof, A.L., 1984. EMG and Muscle Force: An Introduction. Hum. Mov. Sci. 3, 119–153.

Hogan, M.E., Taddio, A., Katz, J., Shah, V., Krahn, M., 2016. Incremental health care costs for chronic pain in Ontario, Canada: A population-based matched cohort study of adolescents and adults using administrative data. Pain 157, 1626–1633. https://doi.org/10.1097/j.pain.0000000000000561

Huxley, A.F., Niedergerke, R., 1954. Structural changes in muscle during contraction. Nature 4412, 971–973.

Iridiastadi, H., Nussbaum, M.A., 2006. Muscular Fatigue and Endurance During Intermittent Static Efforts : Effects of Contraction Level , Duty Cycle , and Cycle Time. Hum. Factors 48, 710–720.

Jones, D.A., 1996. High- and low-frequency fatigue revisited. Acta Physiol. Scand. 156, 265–270. https://doi.org/10.1046/j.1365-201X.1996.192000.x

Jones, T., Kumar, S., 2010. Comparison of ergonomic risk assessment output in four sawmill jobs. Int. J. Occup. Saf. Ergon. 16, 105–111. https://doi.org/10.1080/10803548.2010.11076834

Kernell, D., Monster, A.W., 1982. Motoneurone properties and motor fatigue - An intracellular

study of gastrocnemius motoneurones of the cat. Exp. Brain Res. 46, 197–204. https://doi.org/10.1007/BF00237177

Kumar, S., 2001. Theories of musculoskeletal injury causation. Ergonomics 44, 17–47. https://doi.org/10.1080/00140130120716

Lowe, B.D., Dempsey, P.G., Jones, E.M., 2019. Ergonomics assessment methods used by ergonomics professionals. Appl. Ergon. 81, 102882. https://doi.org/10.1016/j.apergo.2019.102882

Lucas-Osma, A.M., Collazos-Castro, J.E., 2009. Compartmentalization in the triceps brachii motoneuron nucleus and its relation to muscle architecture. J. Comp. Neurol. 516, 226–239. https://doi.org/10.1002/cne.22123

Lymn, R.W., Taylor, E.W., 1971. Mechanism of Adenosine Triphosphate Hydrolysis by Actomyosin. Biochemistry 10, 4617–4624. https://doi.org/10.1021/bi00801a004

Machado, A.F., Evangelista, A.L., Miranda, J.M. de Q., Teixeira, C.V.L.S., Leite, G. dos S., Rica, R.L., Figueira Junior, A., Baker, J.S., Bocalini, D.S., 2018. Sweat rate measurements after high intensity interval training using body weight. Rev. Bras. Med. do Esporte 24, 197–201. https://doi.org/10.1590/1517-869220182403178641

McFadden, L.K., McComas, A.J., 1996. Late depression of muscle excitability in humans after fatiguing stimulation. J. Physiol. 496, 851–855. https://doi.org/10.1113/jphysiol.1996.sp021732

McKenzie, D.K., Bigland-Ritchie, B., Gorman, R.B., Gandevia, S.C., 1992. Central and peripheral fatigue of human diaphragm and limb muscles assessed by twitch interpolation. J. Physiol. 454, 643–656. https://doi.org/10.1113/jphysiol.1992.sp019284

Mehdizadeh, A., Vinel, A., Hu, Q., Schall, M.C., Gallagher, S., Sesek, R.F., 2020. Job rotation and work-related musculoskeletal disorders: a fatigue-failure perspective. Ergonomics 63, 461–476. https://doi.org/10.1080/00140139.2020.1717644

Miyamoto, N., Fukutani, A., Yanai, T., Kawakami, Y., 2012. Twitch potentiation after voluntary contraction and neuromuscular electrical stimulation at various frequencies in human quadriceps femoris. Muscle and Nerve 45, 110–115. https://doi.org/10.1002/mus.22259

Moxham, J., Edwards, R.H.T., Aubier, M., De Troyer, A., Farkas, G., Macklem, P.T., Roussos, C., 1982. Changes in EMG power spectrum (high-to-low ratio) with force fatigue in humans. J. Appl. Physiol. Respir. Environ. Exerc. Physiol. 53, 1094–1099. https://doi.org/10.1152/jappl.1982.53.5.1094

Neumann, W.P., Motiwala, M., Rose, L.M., 2020. A comparison of work-rest models using a “breakpoint” analysis raises questions. IISE Trans. Occup. Ergon. Hum. Factors 0, 1–11. https://doi.org/10.1080/24725838.2020.1857315

Pallant, J., 2011. Statistic material for English International Learners (EIL) SPSS Survival Manual A Step by Step Guide to Data.

Potvin, J.R., Fuglevand, A.J., 2018. A motor unit-based model of muscle fatigue and recovery, in: Abstracts, Presentations, International Society of Electrophysiology and Kinesiology.

International Society of Electrophysiology and Kinesiology, Dublin, Ireland, p. 144. [O18.4]. https://doi.org/10.1371/journal.pcbi.1005581

Potvin, J.R., Fuglevand, A.J., 2017a. A motor unit-based model of muscle fatigue. PLoS Comput Biol 13, e1005581. https://doi.org/10.1371/journal.pcbi.1005581

Potvin, J.R., Fuglevand, A.J., 2017b. A motor unit-based model of muscle fatigue. PLoS Comput. Biol. 13. https://doi.org/10.1371/journal.pcbi.1005581

Rashedi, E., Nussbaum, M.A., 2016. Cycle time influences the development of muscle fatigue at low to moderate levels of intermittent muscle contraction. J. Electromyogr. Kinesiol. 28, 37–45. https://doi.org/10.1016/j.jelekin.2016.03.001

Roberts, M.F., Wenger, C.B., Stolwijk, J.A.J., Nadel, E.R., 1977. Skin blood flow and sweating changes following exercise training and heat acclimation. J. Appl. Physiol. Respir. Environ. Exerc. Physiol. 43, 133–137. https://doi.org/10.1152/jappl.1977.43.1.133

Shield, A., Zhou, S., 2004. Assessing Voluntary Muscle Activation with the Twitch Interpolation Technique. Sport. Med. 34, 253–267.

Shorrock, S.T., Williams, C.A., 2016. Human factors and ergonomics methods in practice: three fundamental constraints. Theor. Issues Ergon. Sci. 17, 468–482. https://doi.org/10.1080/1463922X.2016.1155240

Smith, I.C., Gittings, W., Huang, J., McMillan, E.M., Quadrilatero, J., Tupling, R.R., Vandenboom, R., 2013. Potentiation in mouse lumbrical muscle without myosin light chain phosphorylation: Is resting calcium responsible? J. Gen. Physiol. 141, 297–308. https://doi.org/10.1085/jgp.201210918

Suga, T., Okita, K., Takada, S., Omokawa, M., Kadoguchi, T., Yokota, T., Hirabayashi, K., Takahashi, M., Morita, N., Horiuchi, M., Kinugawa, S., Tsutsui, H., 2012. Effect of multiple set on intramuscular metabolic stress during low-intensity resistance exercise with blood flow restriction. Eur. J. Appl. Physiol. 112, 3915–3920. https://doi.org/10.1007/s00421-012-2377-x

Takatani, K.C., Bruchal, L.C., 2017. A new approach to prevent overuse injuries of the rotator cuff supraspinatus tendon using the cumulative fatigue concept. Theor. Issues Ergon. Sci. 18, 455–475. https://doi.org/10.1080/1463922X.2017.1284281

Tupling, R., Green, H., Grant, S., Burnett, M., Ranney, D., 2000. Postcontractile force depression in humans is associated with an impairment in SR Ca2+ pump function. Am. J. Physiol. - Regul. Integr. Comp. Physiol. 278, 87–94. https://doi.org/10.1152/ajpregu.2000.278.1.r87

Uttley, J., 2019. Power Analysis, Sample Size, and Assessment of Statistical Assumptions—Improving the Evidential Value of Lighting Research. LEUKOS - J. Illum. Eng. Soc. North Am. 15, 143–162. https://doi.org/10.1080/15502724.2018.1533851

Veerasammy, S., Davidson, J.B., Fischer, S.L., 2022. Multi-task exposure assessment to infer musculoskeletal disorder risk: A scoping review of injury causation theories and tools available to assess exposures. Appl. Ergon. 102, 103766. https://doi.org/10.1016/j.apergo.2022.103766

Veiersted, K.B., Westgaard, R.H., Andersen, P., 1990. Pattern of muscle activity during stereotyped work and its relation to muscle pain. Int. Arch. Occup. Environ. Health 61, 31–41. https://doi.org/10.1007/BF00397846

Visser, B, Van Dieën, J.H., 2006. Pathophysiology of upper extremity muscle disorders. J. Electromyogr. Kinesiol. 16, 1–16. https://doi.org/10.1016/j.jelekin.2005.06.005

Visser, Bart, Van Dieën, J.H., 2006. Pathophysiology of upper extremity muscle disorders. J. Electromyogr. Kinesiol. 16, 1–16. https://doi.org/10.1016/j.jelekin.2005.06.005

Vøllestad, N.K., 1997. Measurement of human muscle fatigue. J. Neurosci. Methods 74, 219–227. https://doi.org/10.1016/S0165-0270(97)02251-6

Wells, R., Van Eerd, D., Hägg, G., 2004. Mechanical exposure concepts using force as the agent. Scand. J. Work. Environ. Heal. 30, 179–190. https://doi.org/10.5271/sjweh.778

Yung, M., 2016. Fatigue at the Workplace : Measurement and Temporal Development by. Thesis.

Yung, M., Bigelow, P.L., Hastings, D.M., Wells, R.P., 2014. Detecting within- and between-day manifestations of neuromuscular fatigue at work: an exploratory study. Ergonomics 57, 1562–1573. https://doi.org/10.1080/00140139.2014.934299

Yung, M., Mathiassen, S.E., Wells, R.P., 2012. Variation of force amplitude and its effects on local fatigue. Eur. J. Appl. Physiol. 112, 3865–3879. https://doi.org/10.1007/s00421-012-2375-z

Yung, M., Wells, R.P., 2017. Documenting the Temporal Pattern of Fatigue Development. IISE Trans. Occup. Ergon. Hum. Factors 5, 115–135. https://doi.org/10.1080/24725838.2017.1373714

Appendix

Appendix A: Get Active Questionnaire

Get Active Questionnaire

CANADIAN SOCIETY FOR EXERCISE PHYSIOLOGY –
PHYSICAL ACTIVITY TRAINING FOR HEALTH (CSEP-PATH®)

Physical activity improves your physical and mental health. Even small amounts of physical activity are good, and more is better.

For almost everyone, the benefits of physical activity far outweigh any risks. For some individuals, specific advice from a Qualified Exercise Professional (QEP – has post-secondary education in exercise sciences and an advanced certification in the area – see csep.ca/certifications) or health care provider is advisable. **This questionnaire is intended for all ages – to help move you along the path to becoming more physically active.**

☐ I am completing this questionnaire for myself.

☐ I am completing this questionnaire for my child/dependent as parent/guardian.

PREPARE TO BECOME MORE ACTIVE

The following questions will help to ensure that you have a safe physical activity experience. Please answer **YES** or **NO** to each question before you become more physically active. If you are unsure about any question, answer **YES**.

YES	NO	
		1 Have you experienced **ANY** of the following (A to F) **within the past six months**?
●	●	**A** A diagnosis of/treatment for heart disease or stroke, or pain/discomfort/pressure in your chest during activities of daily living or during physical activity?
●	●	**B** A diagnosis of/treatment for high blood pressure (BP), or a resting BP of 160/90 mmHg or higher?
●	●	**C** Dizziness or lightheadedness during physical activity?
●	●	**D** Shortness of breath at rest?
●	●	**E** Loss of consciousness/fainting for any reason?
●	●	**F** Concussion?
●	●	**2** Do you currently have pain or swelling in any part of your body (such as from an injury, acute flare-up of arthritis, or back pain) that affects your ability to be physically active?
●	●	**3** Has a health care provider told you that you should avoid or modify certain types of physical activity?
●	●	**4** Do you have any other medical or physical condition (such as diabetes, cancer, osteoporosis, asthma, spinal cord injury) that may affect your ability to be physically active?

NO to all questions: go to Page 2 – ASSESS YOUR CURRENT PHYSICAL ACTIVITY

YES to any question: go to Reference Document – ADVICE ON WHAT TO DO IF YOU HAVE A YES RESPONSE

PAGE 1 OF 2

Get Active Questionnaire

ASSESS YOUR CURRENT PHYSICAL ACTIVITY

Answer the following questions to assess how active you are now.

1 During a typical week, on how many days do you do moderate- to vigorous-intensity aerobic physical activity (such as brisk walking, cycling or jogging)? ____ DAYS/WEEK

2 On days that you do at least moderate-intensity aerobic physical activity (e.g., brisk walking), for how many minutes do you do this activity? ____ MINUTES/DAY

For adults, please multiply your average number of days/week by the average number of minutes/day: ____ MINUTES/WEEK

Canadian Physical Activity Guidelines recommend that adults accumulate at least 150 minutes of moderate- to vigorous-intensity physical activity per week. For children and youth, at least 60 minutes daily is recommended. Strengthening muscles and bones at least two times per week for adults, and three times per week for children and youth, is also recommended (see csep.ca/guidelines).

GENERAL ADVICE FOR BECOMING MORE ACTIVE

Increase your physical activity gradually so that you have a positive experience. Build physical activities that you enjoy into your day (e.g., take a walk with a friend, ride your bike to school or work) and reduce your sedentary behaviour (e.g., prolonged sitting).

If you want to do **vigorous-intensity physical activity** (i.e., physical activity at an intensity that makes it hard to carry on a conversation), and you do not meet minimum physical activity recommendations noted above, consult a Qualified Exercise Professional (QEP) beforehand. This can help ensure that your physical activity is safe and suitable for your circumstances.

Physical activity is also an important part of a healthy pregnancy.

Delay becoming more active if you are not feeling well because of a temporary illness.

DECLARATION

To the best of my knowledge, all of the information I have supplied on this questionnaire is correct. If my health changes, I will complete this questionnaire again.

I answered NO to all questions on Page 1

Sign and date the Declaration below

I answered YES to any question on Page 1

Check the box below that applies to you:

- ☐ I have consulted a health care provider or Qualified Exercise Professional (QEP) who has recommended that I become more physically active.
- ☐ I am comfortable with becoming more physically active on my own without consulting a health care provider or QEP.

Name (+ Name of Parent/Guardian if applicable) [Please print]	Signature (or Signature of Parent/Guardian if applicable)	Date of Birth

Date	Email (optional)	Telephone (optional)

With planning and support you can enjoy the benefits of becoming more physically active. A QEP can help.

☐ Check this box if you would like to consult a QEP about becoming more physically active.
(This completed questionnaire will help the QEP get to know you and understand your needs.)

Appendix B: Nordic Musculoskeletal Questionnaire

Mine: ___

Initial of first name: __ Initial of last name: __ Last 4 digits of social security number: __ __ __ __ Immediate Supervisor: _____ Date: ___/___/___

Job Title: _____ Section: _____ Gender: M F Age: _____ Height: ___ ft.___ in. Weight: _____

How long have you been doing this job? _____ years _____ months On average, how many hours do you work each week? _____

To be answered by everyone		To be answered by those who have had trouble	
Have you at any time during **the last 12 months** had trouble (ache, pain, discomfort, numbness) in:		Have you at any time during the **last 12 months been prevented from doing your normal work** (at home or away from home) because of the trouble?	Have you had trouble at any time during **the last 7 days?**
Neck	☐ Yes	☐ No ☐ Yes	☐ No ☐ Yes
Shoulders			
☐ No	☐ Yes, right shoulder ☐ Yes, left shoulder ☐ Yes, both shoulders	☐ No ☐ Yes	☐ No ☐ Yes
Elbows			
☐ No	☐ Yes, right elbow ☐ Yes, left elbow ☐ Yes, both elbows	☐ No ☐ Yes	☐ No ☐ Yes
Wrists/Hands			
☐ No	☐ Yes, right wrist/hand ☐ Yes, left wrist/hand ☐ Yes, both wrists/hands	☐ No ☐ Yes	☐ No ☐ Yes
Upper Back			
☐ No	☐ Yes	☐ No ☐ Yes	☐ No ☐ Yes
Lower Back (small of back)			
☐ No	☐ Yes	☐ No ☐ Yes	☐ No ☐ Yes
One or Both Hips/Thighs			
☐ No	☐ Yes	☐ No ☐ Yes	☐ No ☐ Yes
One or Both Knees			
☐ No	☐ Yes	☐ No ☐ Yes	☐ No ☐ Yes
One or Both Ankles/Feet			
☐ No	☐ Yes	☐ No ☐ Yes	☐ No ☐ Yes

***Based on the Nordic Questionnaire**

Appendix C: Absolute and Normalized Overall Mean Force Responses

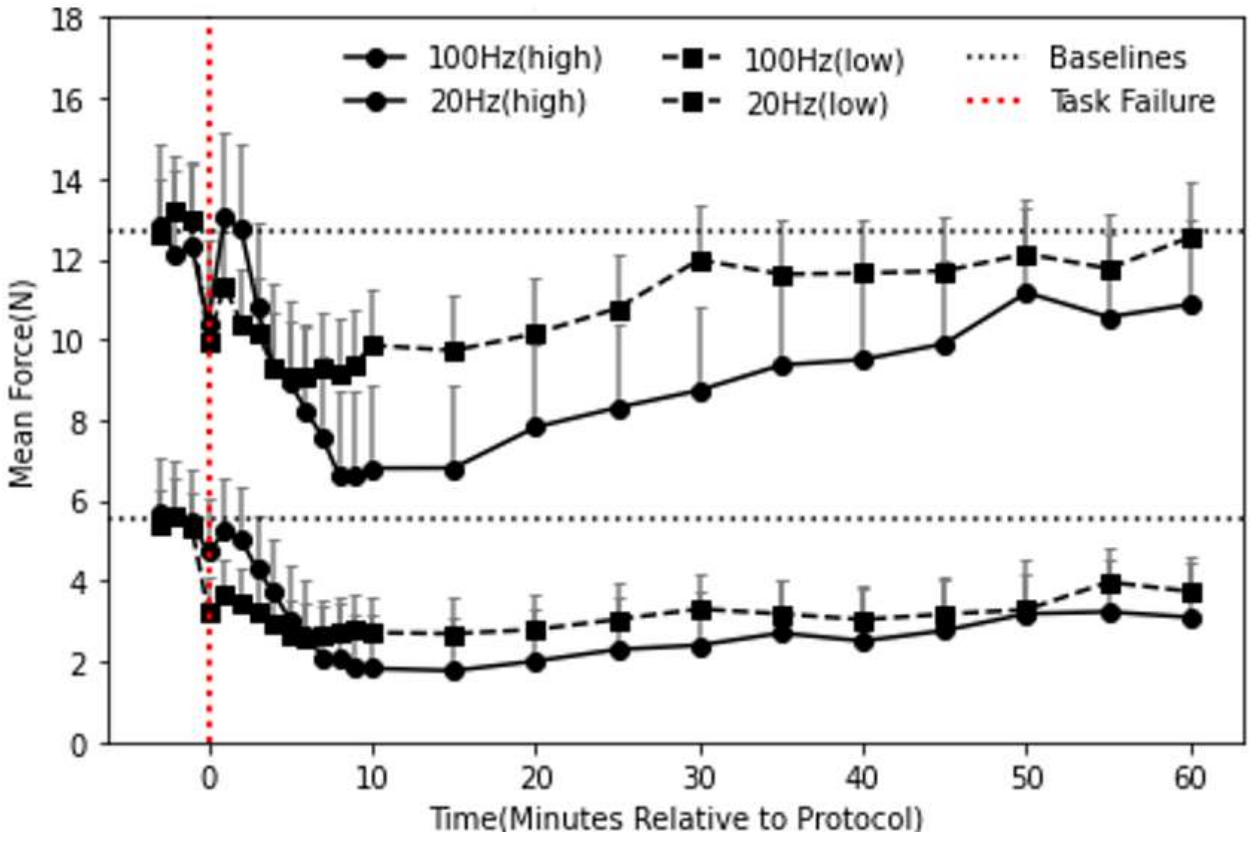

Figure 30: Absolute mean force responses from 100 Hz and 20 Hz stimulation frequencies across high and low intensities

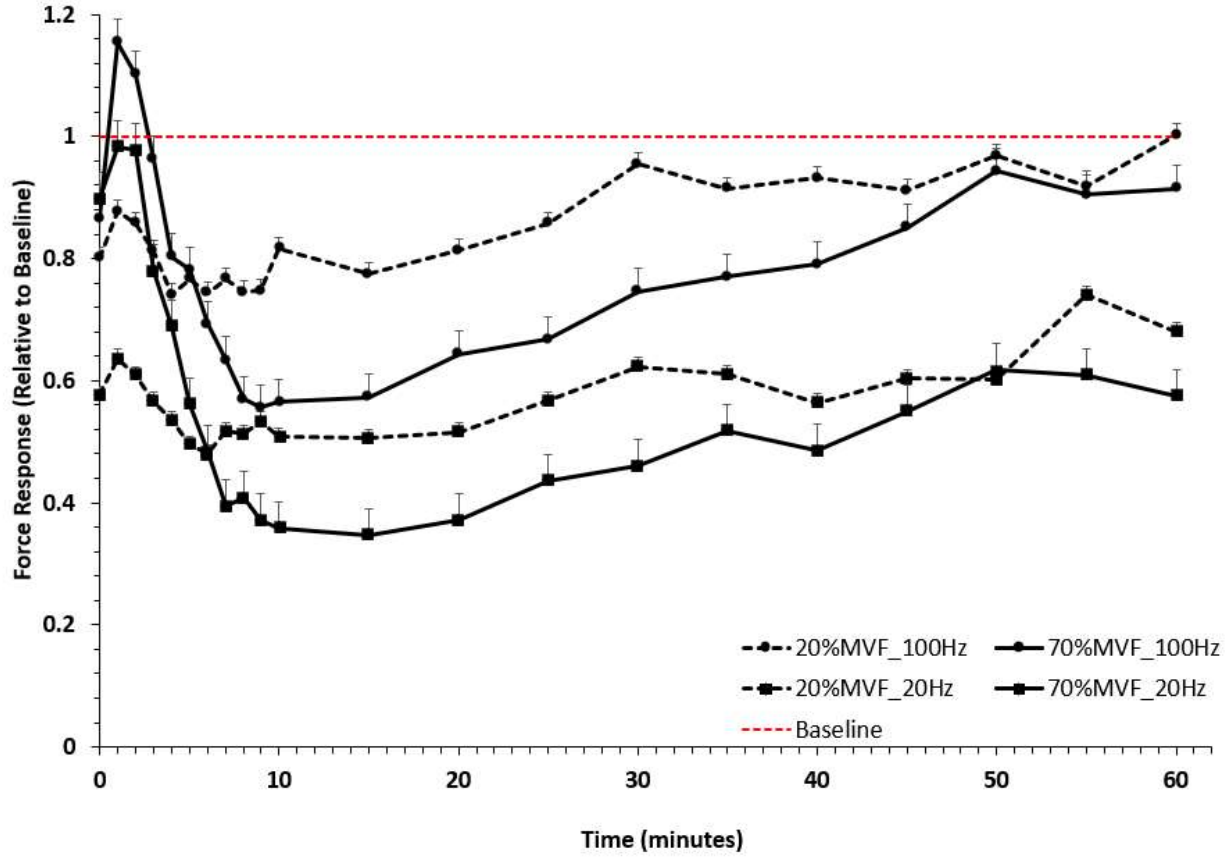

Figure 31: Normalized mean force responses from 100 Hz and 20 Hz stimulation frequencies across high and low intensities

Appendix D: Detailed Statistical Results from Pairwise Comparisons

Table 7: Results from the pairwise comparisons of normalized force responses at high and low intensities to baseline across time

	70 %MVF		20 %MVF	
Baseline versus Time (Minutes)	**Adjusted p value**	**Significance**	**Adjusted p value**	**Significance**
0	1.000	ns	$p < 0.001$	*
1	1.000	ns	0.002	*
2	1.000	ns	$p < 0.001$	*
3	1.000	ns	$p < 0.001$	*
4	$p < 0.001$	*	$p < 0.001$	*
5	$p < 0.001$	*	$p < 0.001$	*
6	$p < 0.001$	*	$p < 0.001$	*
7	$p < 0.001$	*	$p < 0.001$	*
8	$p < 0.001$	*	$p < 0.001$	*
9	$p < 0.001$	*	$p < 0.001$	*
10	$p < 0.001$	*	$p < 0.001$	*
15	$p < 0.001$	*	$p < 0.001$	*
20	$p < 0.001$	*	$p < 0.001$	*
25	$p < 0.001$	*	$p < 0.001$	*
30	$p < 0.001$	*	0.042	*
35	$p < 0.001$	*	$p < 0.001$	*
40	$p < 0.001$	*	$p < 0.001$	*
45	$p < 0.001$	*	$p < 0.001$	*
50	0.013	*	0.007	*
55	0.002	*	0.094	ns
60	$p < 0.001$	*	0.360	ns

Table 8: Results of the pairwise comparisons of normalized force responses between high and low intensities across time

Time (minutes)	**Adjusted p value (70 %MVF vs 20 %MVF)**	**Significance**
0	0.001	*
1	$p < 0.001$	*
2	$p < 0.001$	*
3	0.004	*
4	0.030	*
5	0.429	ns
6	0.622	ns
7	0.009	*
8	0.006	*
9	$p < 0.001$	*
10	0.001	*
15	$p < 0.001$	*
20	0.001	*
25	0.004	*
30	0.003	*
35	0.078	ns
40	0.049	*
45	0.281	ns
50	0.921	ns
55	0.249	ns
60	0.046	*

Table 9: Results from the pairwise comparisons of normalized force responses at high and low frequencies to baseline across time

	100 Hz		20 Hz	
Baseline versus Time (Minutes)	**Adjusted p value**	**Significance**	**Adjusted p value**	**Significance**
0	0.027	*	$p < 0.001$	*
1	1.00	ns	0.044	*
2	1.00	ns	0.169	ns
3	1.00	ns	$p < 0.001$	*
4	$p < 0.001$	*	$p < 0.001$	*
5	$p < 0.001$	*	$p < 0.001$	*
6	$p < 0.001$	*	$p < 0.001$	*
7	$p < 0.001$	*	$p < 0.001$	*
8	$p < 0.001$	*	$p < 0.001$	*
9	$p < 0.001$	*	$p < 0.001$	*
10	$p < 0.001$	*	$p < 0.001$	*
15	$p < 0.001$	*	$p < 0.001$	*
20	$p < 0.001$	*	$p < 0.001$	*
25	$p < 0.001$	*	$p < 0.001$	*
30	0.531	ns	$p < 0.001$	*
35	0.15	ns	$p < 0.001$	*
40	0.22	ns	$p < 0.001$	*
45	0.95	ns	$p < 0.001$	*
50	1.00	ns	$p < 0.001$	*
55	1.00	ns	$p < 0.001$	*
60	1.00	ns	$p < 0.001$	*

Table 10: Results of the pairwise comparisons of normalized force between high and low frequencies across time

Time	Adjusted p value (100 Hz vs 20 Hz)	Significance
0	0.043	*
1	$p < 0.001$	*
2	$p < 0.001$	*
3	$p < 0.001$	*
4	$p < 0.001$	*
5	$p < 0.001$	*
6	$p < 0.001$	*
7	$p < 0.001$	*
8	$p < 0.001$	*
9	$p < 0.001$	*
10	$p < 0.001$	*
15	$p < 0.001$	*
20	$p < 0.001$	*
25	$p < 0.001$	*
30	$p < 0.001$	*
35	$p < 0.001$	*
40	$p < 0.001$	*
45	$p < 0.001$	*
50	$p < 0.001$	*
55	$p < 0.001$	*
60	$p < 0.001$	*

Appendix E: Average Normalized Force Response across all frequencies and intensities

Table 11: Average Normalized Force Response following the low intensity (20%MVF) and high intensity (70%MVF) protocols

	Normalized Force Response (n = 28)			
Time (mins)	20%MVF/100Hz	70%MVF/100Hz	20%MVF/20Hz	70%MVF/20Hz
0	0.800	0.866	0.577	0.899
1	0.877	1.154	0.637	0.983
2	0.857	1.102	0.609	0.979
3	0.811	0.962	0.566	0.779
4	0.741	0.803	0.535	0.689
5	0.766	0.781	0.495	0.561
6	0.743	0.693	0.480	0.483
7	0.767	0.634	0.517	0.394
8	0.745	0.569	0.513	0.409
9	0.748	0.556	0.534	0.371
10	0.817	0.565	0.508	0.359
15	0.776	0.573	0.506	0.347
20	0.813	0.643	0.516	0.371
25	0.858	0.667	0.567	0.435
30	0.956	0.746	0.623	0.46
35	0.914	0.77	0.611	0.518
40	0.933	0.79	0.564	0.485
45	0.912	0.851	0.604	0.55
50	0.968	0.943	0.603	0.617
55	0.919	0.905	0.74	0.609
60	1.002	0.915	0.68	0.575
Standard Deviation	0.083	0.173	0.066	0.198

Appendix F: Percent activation across high and low intensity protocols

Table 12: Average percent activation of the long and lateral heads of the triceps brachii, and of the biceps brachii, during the high intensity protocol (70%MVF)

Time (%Endurance Time)	Force (%MVF)	Long Head Activation (%MVC)	Lateral Head Activation (%MVC)	Biceps Activation (%MVC)
1	23.43	15.18	14.86	1.43
5	53.41	35.95	35.98	3.49
10	59.98	41.56	41.56	4.07
20	67.33	50.80	51.30	5.27
30	66.89	52.28	53.70	5.55
40	67.28	52.44	53.67	5.54
50	67.93	54.71	57.17	5.68
60	67.06	55.37	59.47	5.66
70	66.69	55.51	60.99	5.64
80	64.65	55.71	62.22	5.71
90	63.23	51.70	61.39	5.45
100	41.31	38.14	45.94	4.19
Standard Deviation	13.70	12.11	13.78	1.31

Table 13: Average percent activation of the long and lateral heads of the triceps brachii, and of the biceps brachii, during the low intensity protocol (20%MVF)

Time (%Endurance Time)	Force (%MVF)	Long Head Activation (%MVC)	Lateral Head Activation (%MVC)	Biceps Activation (%MVC)
12.5	19.73	8.93	8.87	1.04
25	19.61	8.65	9.82	1.20
37.5	19.57	9.63	10.59	1.16
50	19.50	10.73	12.40	1.22
62.5	19.65	12.83	14.21	1.47
75	19.58	15.31	16.88	1.76
87.5	19.46	15.53	18.25	1.72
100	19.02	21.11	20.56	2.09